X-643-65-40

NASA TMX-55128

IMP-C
ORBIT AND LAUNCH TIME ANALYSIS

BY

STEPHEN J. PADDACK

BARBARA E. SHUTE

JANUARY 1965

GODDARD SPACE FLIGHT CENTER

GREENBELT, MARYLAND

X-643-65-40

IMP-C

ORBIT AND LAUNCH TIME ANALYSIS

by

Stephen J. Paddack and Barbara E. Shute
Special Projects Branch
Theoretical Division

January 1965

Goddard Space Flight Center
Greenbelt, Maryland

TABLE OF CONTENTS

Page

LIST OF SKETCHES

LIST OF ILLUSTRATIONS

LIST OF TABLES

NOMENCLATURE

a	Semi-major axis
E.S.T.	Eastern Standard Time
e	Eccentricity
G	Gravitational constant
i	Inclination
M_E	Mass of the earth
RA	Right ascension
t	Time
U.T.	Universal Time
v	Magnitude of velocity vector
x_p, y_p, z_p	Coordinates of perigee
x_s, y_s, z_s	Coordinates of sun
$\overline{1}_p$	Unit vector to perigee
$\overline{1}_s$	Unit vector to sun
α	Apogee-sun angle
β	Spin axis – ecliptic plane angle
δ	Declination
δ_a	Declination of apogee
λ	Spin axis – sun angle
μ	Earth's gravitational constant
σ	Defined by equation (3)
Ω	Right ascension of ascending node
Ω_0	Initial value of Ω
ω	Argument of perigee

IMP-C

ORBIT AND LAUNCH TIME ANALYSIS

ABSTRACT

The purpose of this document is to show the time available for launch of the IMP-C satellite in order to obtain a successful mission. The analysis assumes that the rocket that places the satellite in orbit operates within acceptable tolerances. The launch time available is then dominated by the restraints imposed on the mission. In the case of the IMP-C four restraints are considered: lifetime, two restraints on orientation in space and the anticipated amount of time spent in the shadow of the earth or moon. Lifetime and one of the orientation restraints are mandatory and the other two restraints are desired. The resulting time available for launch satisfying these conditions is shown. This time period (or periods) is defined as the launch window. The result is shown on a launch window map and also in tabular form. The analysis takes into account the anticipated dispersion on injection speed and also the high frequency perturbative effects of the moon. The successful use of an analog computer program is disclosed.

Author

IMP-C
ORBIT AND LAUNCH TIME ANALYSIS

INTRODUCTION

The Interplanetary Monitoring Platform (IMP) satellites belong to a family of satellites which are designed to carry out experiments in near earth and cislunar space. The orbits for the IMP's are highly eccentric (i.e., $e > 0.7$). In this document the orbit for the IMP-C is analyzed to find the times available for successful launch. The period (or periods) of time available for successful launch is defined as the launch window. The success or failure of a mission of this nature is related to lifetime and also to suitable spacecraft orientation in space for the proper operation of the experiments. The failure of a mission in regard to lifetime is caused by the orbit being placed in space such that forces act on the satellite which cause it to pass through the dense atmosphere and be destroyed. A failure in regard to spacecraft orientation occurs when the satellite simply doesn't "look" in the right direction in space even though the orbit itself may be suitably placed in space. The analysis in this document assumes that the rocket used to place the IMP-C in orbit will operate successfully.

The conditions that must be met in order to have a successful mission are defined as the mandatory restraints. Often there are restraints which are desired but not mandatory. In the case of the IMP-C there are two mandatory restraints and two desired restraints. The four restraints are summarized below:

1. Lifetime, at least one year (mandatory).
2. Spin axis-sun angle between specified limits (mandatory).
3. Time in shadow not to exceed certain limits (desired).
4. Apogee-sun angle below a specified value and decreasing (desired).

The launch window consistent with the above four restraints is shown in this document.

I. ASSUMPTIONS

A. Nominal Initial Orbits

Three basic orbits are taken into consideration in this investigation for the IMP-C satellite. These orbits differ principally in apogee height. The approximate values of the initial apogee height are 110,000 n.m., 120,000 n.m. and 140,000 n.m.

A set of firm injection conditions exist for the 110K n.m. case at this writing. The injection conditions for the 120K n.m. and 140K n.m. cases are calculated by varying the injection speed and retaining the other injection conditions from the 110K n.m. case. The parameters which are considered constant are the injection sub-satellite position (i.e. latitude and longitude), the injection height, the azimuth and the elevation angle. The injection speeds for the 120K n.m. and 140K n.m. orbits are calculated from the "vis-viva" integral:

$$v^2 = GM_E \left[\frac{2}{r} - \frac{1}{a}\right] \tag{1}$$

where v = magnitude of injection velocity

G = gravitational constant

M_E = mass of earth

r = radius distance to satellite

a = semi-major axis.

Since this equation assumes a Keplerian orbit, the injection speed is slightly adjusted in order to attain the desired apogee height because of the perturbations on the orbit.

It is realized that for the different orbits the other injection conditions change somewhat, but, usually, this change is small. The effect of assuming these to be constant is small and considered negligible in a survey of this nature.

The classical orbital elements associated with each of the above injection conditions are shown in Table II. These elements are the osculating elements which are obtained from the injection conditions by an Encke method numerical integration program (ITEM, Ref. 1). The selection of the elements is discussed in Section II-E of this document.

Table I
IMP-C Injection Conditions

Apogee Heights	110K n.m.	120K n.m.	140K n.m.
Latitude (geodetic)	$23^\circ.268$ N	$23^\circ.268$ N	$23^\circ.268$ N
Longitude	$66^\circ.714$ W	$66^\circ.714$ W	$66^\circ.714$ W
Height	194.108 km	194.108 km	194.108 km
Speed	10.847832 km/sec	10.8635 km/sec	10.884134 km/sec
Azimuth	$114^\circ.09$	$114^\circ.09$	$114^\circ.09$
Flight Path Angle	$-0^\circ.0004$	$-0^\circ.0004$	$-0^\circ.0004$

Table II
IMP-C Orbital Elements

Apogee Heights	110K n.m.	120K n.m.	140K n.m.
a	16.815218 ER	18.506832 ER	21.343035
e	.93873272	.94433290	.95173037
i	$32^\circ.912693$	$32^\circ.912725$	$32^\circ.912770$
ω	$133^\circ.659044$	$133^\circ.658936$	$133^\circ.658802$
Ω	$197^\circ.445087$	$197^\circ.445087$	$197^\circ.445087$
M	$0^\circ.0$	$0^\circ.0$	$0^\circ.0$
Epoch	1965, 201^d, $7^h.0$	1965, 201^d, $7^h.0$	1965, 201^d, $7^h.0$

In launch window analyses of high eccentricity orbits ($e > .7$) the perigee height is a critical parameter. A relatively small initial perturbation on the orbit can drive the perigee height into dense atmosphere which, of course, would be fatal to the mission. Consequently, in selecting orbital elements care is taken that the injection height and the shape of the orbit are in agreement. This can be expressed mathematically as:

$$\text{Injection height} \simeq a(1-e) \qquad (2)$$

where a and e defined the shape of the orbit.

B. Dispersions on Initial Conditions

The attainment of other than nominal on any of the injection conditions results in an orbit different than the nominal orbit. In view of the fact that injection speed is by far the most dispersed parameter, only the effects of injection speed are investigated. The effects on the lifetime of the dispersions of the other parameters are assumed negligible in comparison with the dispersion on injection speed. The source of injection speed dispersions is assumed to be due solely to the third stage motor.

In order to get a feeling for the speed dispersion on the launching under consideration in this document, the dispersion is approximated by taking the root mean square of the percent of deviation from nominal on the previous ABL X-258 flights, including the IMP-B launching of October 3, 1964, (Ref. 2). The percent of deviation is taken with respect to the nominal speed increment added by the third stage motor. The one-sigma percentage on speed is then defined as:

$$\sigma = \left[\frac{1}{n}\sum\left(\frac{v_n - v_a}{v_n}\,100\right)^2\right]^{1/2} \qquad (3)$$

where n = number of launchings

v_n = nominal injection speed

v_a = actual injection speed

The use of equation (3) is not rigorous but rather produces only an engineering working approximation. When firm values for the dispersion on all parameters exist that portion of the launch window covering the probable launch period should be analyzed again.

C. Restraints on Launch Time

The restraints on the launch time for satellite launchings fall into two basic categories; orbit imposed and spacecraft imposed. The perturbations on a high eccentricity orbit act differently when different launch times are used. Some of these perturbations, for instance the lunar perturbation, affect the orbital lifetime. The lunar perturbation acting adversely drives the perigee height down into the dense atmosphere. Consequently launch times must be selected when the perturbations do not shorten the mission lifetime.

The IMP-C depends on solar energy for power. Hence, long periods in the shadow of the earth may be avoided by proper choice of launch time. The satellite moves slowest at apogee. If the orbit is oriented such that apogee occurs in the earth's shadow then it is possible for the satellite to spend in the order of 13 hours (for the 140K case) in darkness. Therefore, launch times must be chosen such that extended periods in eclipse do not occur.

In regard to the spacecraft imposed restraints there is only one mandatory restraint; that the initial angle between the spin axis and the satellite – sun line be between specified limits. In this case the limits are $30° \leq \lambda \leq 150°$. (Limits of $45° \leq \lambda \leq 135°$ are also considered in this analysis.) This restraint is necessary for the spacecraft experiments. The sketch below shows the spin axis – sun angle, λ.

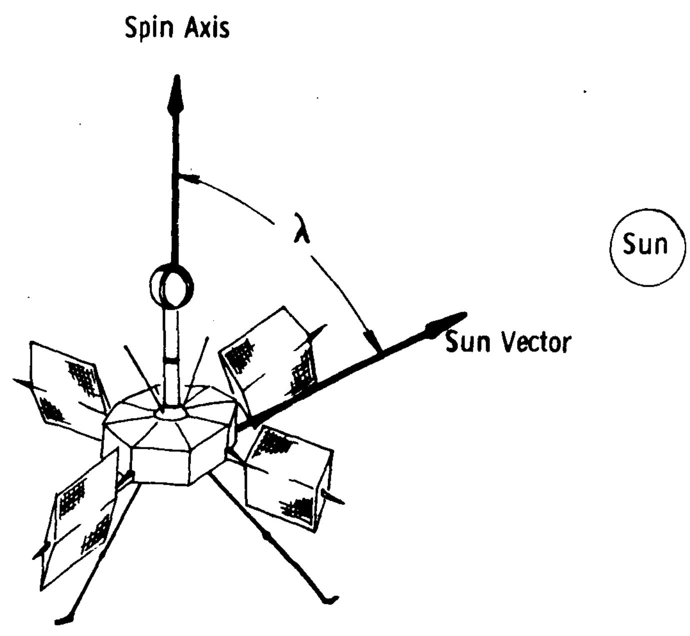

Sketch 1–Spin Axis-Sun Angle, λ

Another experiment imposed restraint is that the initial angle between a vector pointing to apogee from earth's center and the earth sun vector be $< 90°$ and decreasing.

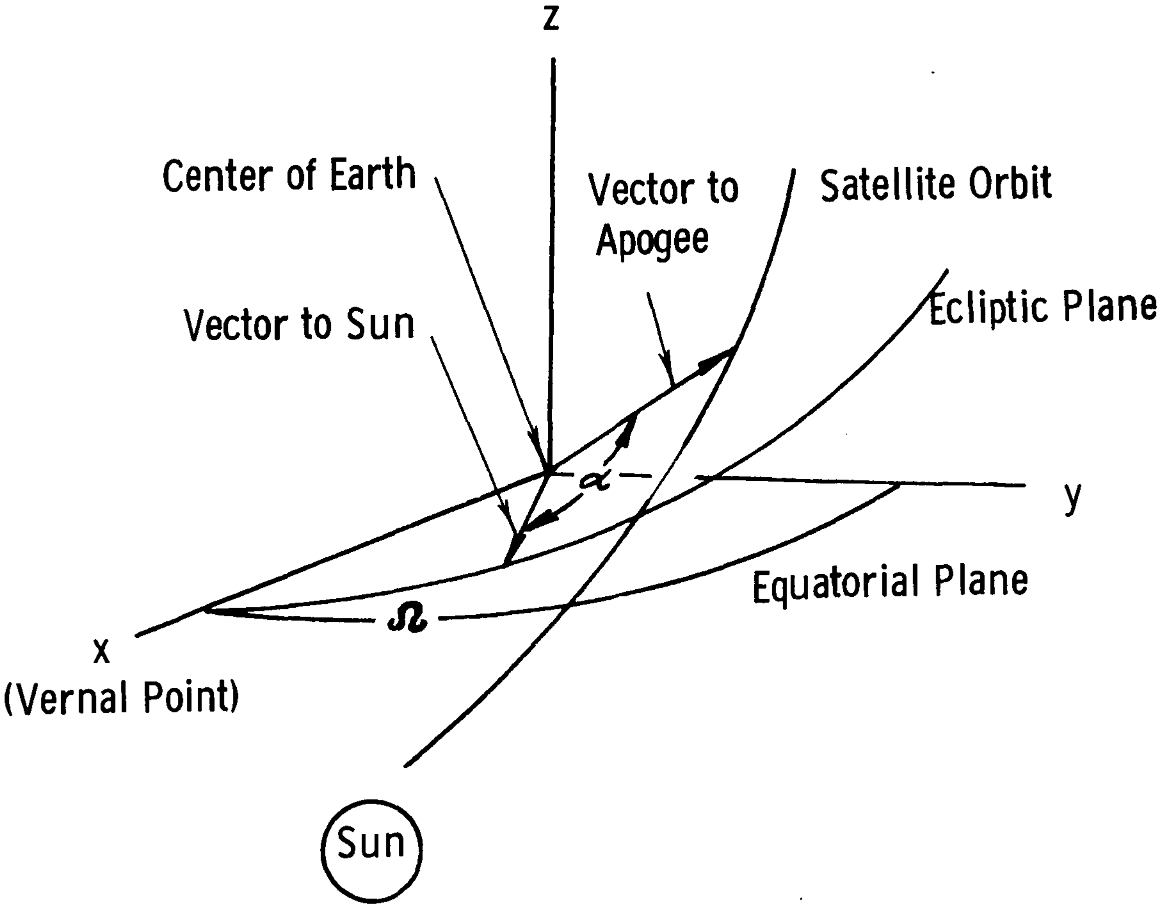

Sketch 2–Apogee-Sun Angle, α

The apogee-sun angle, α is a desirable but not mandatory restraint. The restraints are summarized as follows:

1. Mandatory Restraints.

   a. Maintain one year lifetime (i.e. perigee height not to go below injection height.)

   b. Initial angle between satellite spin axis and satellite sun vector to be between specified limits, either $30° \leq \lambda \leq 150°$ or $45° \leq \lambda \leq 135°$.

2. Desirable Restraints.

   a. Eclipse time not to exceed 3.5 hours for first year or orbital lifetime.

   b. Initial angle between apogee vector and sun vector (earth as origin) to be $<90°$ and decreasing.

II. COMPUTING TECHNIQUES AND PROGRAMS

The launch window map is compiled from a series of numerical integration runs and analog computer runs. Several computer programs are used in order to provide accuracy and to reduce the amount of machine time required.

A. ITEM

The Interplanetary Trajectory Encke Method (ITEM) computer program (Ref. 1) performs a step-by-step numerical integration of the trajectory of the particle in space. It assumes a reference ellipse calculated from the initial conditions using the equations of two-body motion about a spherical earth. Displacements in the position coordinates caused by perturbative forces are calculated by numerical integration and added to the coordinates obtained from the two-body ellipse. This provides the instantaneous position and velocity coordinates of the satellite at time intervals after injection into orbit. These coordinates may be converted into instantaneous elliptical elements called "osculating" elements.

This program has options to compute the effect of several planets, radiation pressure and atmosphere as well as the sun, the moon, and the deviations from sphericity of the earth. It requires about one half hour of machine time to calculate one year's time in orbit. However, the machine time is a function of the integration steps chosen.

B. The Launch Window Program

The Launch Window Program is based on the Halphen method as developed by P. Musen (Ref. 3). The perturbations of the satellite orbital elements by the moon is averaged numerically over the moon's orbital revolution. This program computes the basic long period trend of perigee height with an accuracy comparable to ITEM at a great saving in computer time. It does not consider the oscillations in the perigee height which are introduced by the short period term of the moon.

The Launch Window Program is therefore used to provide orbits with the long term trend of the changes in perigee height for a year; then the ITEM or Analog is used to determine if any of these orbits are unstable due to the high frequency lunar perturbation.

C. The Analog Stability Program

The Analog program developed by Martin Company under NASA contract no. NAS 5-3800 was employed for the first time to develop the launch window maps included in this document. Part of the effort in the development of the launch window presented in this document was performed by the Martin Company under contract NAS 5-9105. Using Moe's equations (Ref. 4), the analog computer draws a year's launch window map with 30 minutes machine time on a comparatively economical machine. The program has the option of operating with or without the short period moon term included. Computation without the moon term is faster and is desirable for preliminary survey purposes. It is possible to use this program to study the size of the launch window assuming the injection conditions to be variable. With the short period moon term in, the program is used for detailed investigations of orbits which, while stable for a year or more from the long period calculations, are terminated early by an unfavorable phase of the short period term.

D. Comparison of the Programs

The changes in the orbital elements of the satellite obtained by the Launch Window Program and by ITEM have been compared previously for IMP, OGO-A, and S-3 satellites (Ref. 5,6). The comparisons show that, with the exception of small oscillatory differences caused by the short period moon term, the results of the two programs agree to several place accuracy over an extended period of time. Exact comparison is limited by the difficulty of choosing analogous starting conditions.

The success of the Analog program in constructing the launch window map is shown by comparison of the boundaries determined by the Launch Window Program and the Analog program. The sawtooth boundary formed by the short period lunar effects falls within the smoother boundary determined by the Launch Window Program which considers long period effects of the moon and sun and the short period effect of the sun as shown on the launch window map on page 25. Further, the Analog Stability Program compares favorably in the detailed map for May with results obtained from ITEM. See Figure 1 for this comparison.

E. Selection of Mean Elements

There is a difference between the way in which orbital elements are defined and used in special perturbation methods and in general perturbations methods. In the Encke method, a special perturbation technique employed in ITEM, the "osculating" elements are obtained by converting the instantaneous cartesian coordinates into elliptical elements using Kepler's Laws for two-body mechanical systems. These elements are subject to comparatively large fluctuations during one orbital period. The oblateness perturbation induces a spike in the orbital elements at perigee (Fig. 2). Satellite orbits with large semi-major axes are highly perturbed when the moon passes nearby. General perturbations methods presently employed in artificial satellite studies such as the Launch Window Program or the Analog Stability Program compute average changes in the orbital elements during one or more orbits. Therefore the initial conditions obtained from the injection parameters do not provide the most suitable "average" orbital elements to be used as input into a general perturbation program. In previous launch window studies, the ITEM program was used to calculate the perturbations from injection until the satellite arrived at the first apogee (Ref. 7). The osculating elements at apogee were used as initial orbital elements to be fed into general perturbation program. This removed the temporary perturbation near the earth caused by the oblateness. However, in an orbit with a large semi-major axis, the moon may strongly perturb the orbit when the satellite reaches the vicinity of apogee. Furthermore, the osculating elements at the first apogee will be markedly different when the injection time is varied because the moon will be in different positions relative to the orbit.

In this study, the osculating elements computed by ITEM one hour after injection were used to represent mean elements for input into general perturbation programs. At this time, the short period effect of the oblateness has disappeared and the lunar and solar perturbations have not begun to have an appreciable effect on the elements. It is advisable to choose elements as nearly "average" as possible in order to obtain good comparisons of the changes in the orbital elements produced by the various computer programs.

III. LAUNCH WINDOW MAPS

A. Year Survey

Figure 3 presents the launch window for all possible launch days and hours from January 1, 1965, to December 31, 1965, based on a nominal 110K n.m. apogee orbit. The abscissa is given in calendar days. The ordinate is given in three equivalent scales: Eastern Standard Time (E.S.T.) at liftoff, Universal Time (U.T.) at liftoff and Universal Time at injection. It is assumed that the rocket flight uses 6.24 minutes between liftoff and injection. The relationship between E.S.T. and U.T. is given by:

$$\text{E.S.T.} = \text{U.T.} - 5 \text{ hours}$$

The hours on the E.S.T. at liftoff ordinate marked with an asterisk (*18.896, *20.896, *22.896 hours) and the hour marked with an asterisk on the U.T. at liftoff ordinate (*23.896) are times which occur the day previous to one being considered in the U.T. at injection scale.

Figure 4 shows a year launch window for the 140K n.m. orbit. This launch window does not show the effect of the high frequency lunar perturbation. It can be seen there is relatively little difference between 140K n.m. orbit launch window and the 120K n.m. orbit launch window when the high frequency moon effect is averaged.

Figure 5 shows a detailed launch window map for the month of May 1965 including $\pm 3\sigma$ effects. This is discussed in Section III-B following.

1. Lifetime Boundary

The smooth outer boundary of Figure 3, the 120K n.m. launch window map, which generally encompasses the "sawtooth" portion of the figure, indicates the launch times available under the assumption that lunar perturbations are averaged such that the perigee height does not go below the injection height for one year of orbital life.

The area contained within the "sawtooth" portion is a more realistic launch window because the short period lunar perturbations are considered. In order to insure a year's orbital life such that perigee heights less than injection height never occur, launch times must be chosen within the "sawtooth" boundary. It can be noted on Figure 3 that there are stringent go no-go situations which often arise. For example, consider the main portion of the launch window during May, June and July: There are days with times during which successful orbits will result interspersed with times where orbits will fail in less than a year, or even less than a month. However, for any given day there is a time when successful launch may occur to satisfy the lifetime restraint.

2. Spacecraft Restraints Boundary

The launch times when the spin axis – sun angle restraint is satisfied lie between the parallel sliding lines shown of the launch window map. The outer dashed lines bound the region where the angle between the spin axis and the sun will always be between 30° and 150°; the inner dashed lines satisfy the more stringent restraint that $45° < \lambda < 135°$. The area bounded by the inner lines lies within the region where the "smoothed" lifetime study indicates satisfactory launches. The upper boundary of the $30° < \lambda < 150°$ requirement is in an area where the orbits are shortlived.

The effect of the eclipse time restraint is also shown on the launch window map. The area above the line running roughly parallel to the upper lifetime boundary, marked with small circles, indicates the launch times which will result in the spacecraft sensing at least 3.5 hours in eclipse at a time during the first year of orbital life. The upward, approximately straight solid lines marked off in this area indicate the number of days which will elapse before the shadow restraint is violated.

Finally, there is the desired, but not mandatory, restraint that the angle α between the apogee vector and sun vector (earth origin) be less than 90° and decreasing. This restraint is not shown explicitly on the year survey launch window map but for any launch time selected from the launch window map the angle α can be determined from Figures 13 through 16. This is discussed in more detail in Sections IV B.

B. Detailed Launch Window Map

In Section I-A of this document it is mentioned that three orbits are under consideration. Usually, in a launch window analysis, the detailed portion is performed last. In this case after the year survey was done, it was decided to launch into a 120K n.m. orbit. Consequently, this detailed analysis is based on the 120K n.m. nominal orbit. The dispersion considered on the injection (initial) conditions is limited to injection speed. The use of equation (3), Section I-B, produced $\sigma = \pm 0.5\%$.

The following apogee heights occurred:

Table III
Apogee Heights $\pm 3\sigma$

	Injection Speed	Apogee Height
$+3\sigma$	11.02645 km/sec.	177,375.7 n.m.
Nominal	10.8635 km/sec.	120,000. n.m.
-3σ	10.70055 km/sec.	89,962.7 n.m.

Also, the perigee height restraint was slightly relaxed from 104.8 n.m. (injection height) to 100.0 n.m.

Figure 5 shows the detailed launch window maps for May 1965. Figure 5 also shows the $\pm 3\sigma$ launch windows, the spin axis-sun angle, λ restraint and the eclipse time restraint. (See Section V-B for more on eclipse time and interpretation.) The spin axis-sun angle, λ restraint was tightened to $45° \leq \lambda \leq 135°$. It is interesting to note that the launch window available which satisfied the spin axis-sun angle restraint is only slightly affected by the dispersion on speed.

IV. SPACECRAFT DATA

A. Spin Axis – Sun Angle, λ

The spin axis-sun angle (λ) is defined to be the angle between the positive spin axis and the vector from the satellite to the sun. The positive spin axis is assumed to be in the direction of the inertial velocity vector of IMP at injection into orbit. The angle, λ is shown in Sketch 1 in Section I-B of this document.

One of the restraints on launch time is that the spin axis – sun angle should be $45° < \lambda < 135°$, or must be at least $30° < \lambda < 150°$. In order to keep within these limits, launch must occur during the band of time bounded by the parallel sliding lines shown on the Launch Window Maps (Figures 3, 5).

Typical behavior curves of the spin axis-sun angle are shown on Figures 6 through 12. The injection times of these curves were chosen from the month of May 1965 to be compatible with the requirements on perigee rise. It may be seen that within these allowed times, a variety of behavior is exhibited. Some of the curves are initially decreasing, some are initially increasing. However, all of the curves oscillate around 90°. The minimums are equivalent to the angle β between the spin axis vector and the ecliptic and the maximums are the complement of β as shown in the sketch on the following page.

The position of the spin axis vector varies along a latitude circle, according to the time of day of launch. A zero value of β is obtained where the latitude circle intersects the ecliptic. In this case, the value of λ will zigzag between 0° and 180° as the sun moves around the ecliptic. When β has a larger value, the value of λ will oscillate in a sinusoidal type curve between β and $180-\beta$ with a period of a year.

It has been assumed in this analysis that there are no forces acting on the spin axis to change the direction of it after the satellite is injected into orbit.

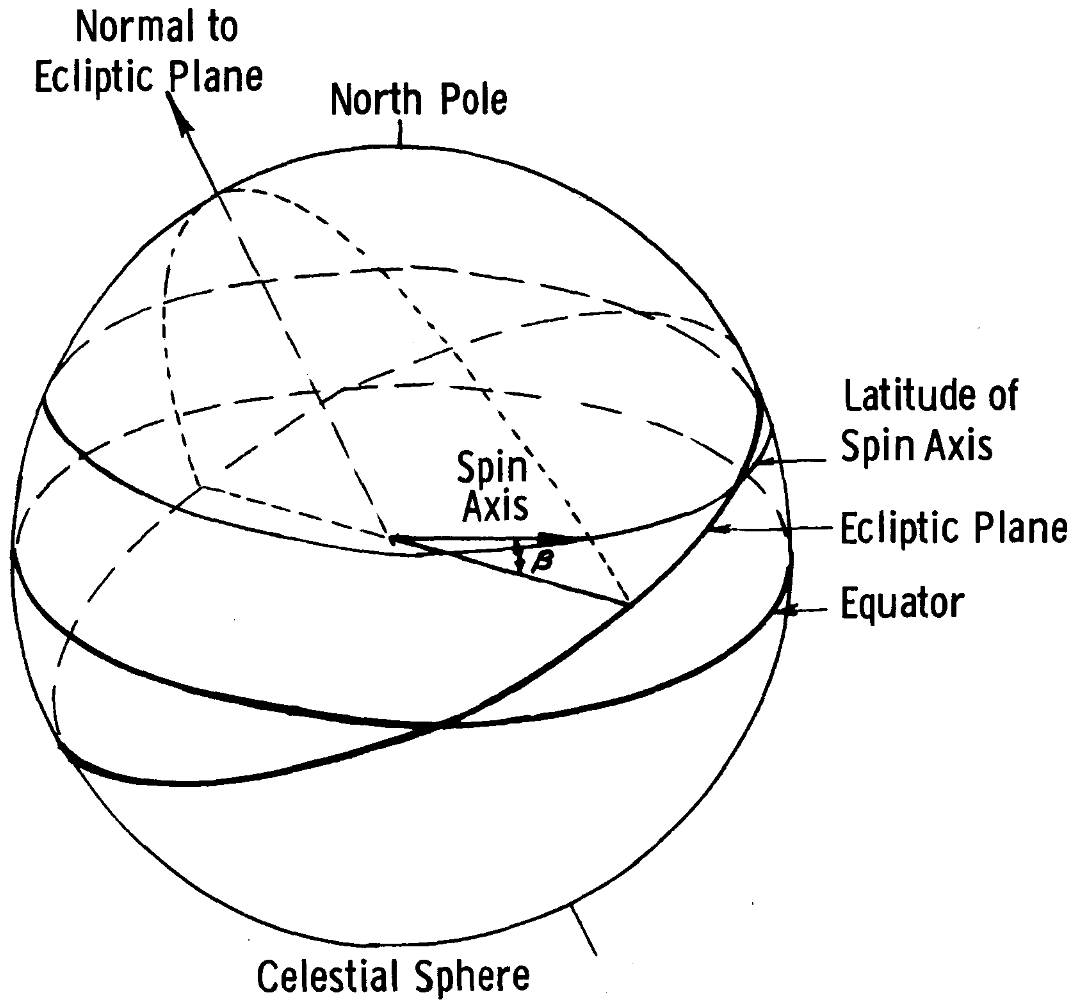

Sketch 3–Spin Axis-Ecliptic Plane Angle, β

B. Apogee-Sun Angle, α

In general the angle α has a sinusoidal type variation with a yearly period. The amplitude of the variation is a function of the initial value of the right ascension of the ascending node, Ω_0 of the satellite's orbit. See Sketch No. 2 in Section II-C.

The XYZ axis system is an inertial reference frame where the X-axis points to the first point of Aires (the vernal point), the Z-axis is the earth's spin axis and points north, the Y-axis completes the right-hand set. Since the earth rotates in this inertial frame the initial value of the node, Ω_0 is solely a function of injection time. Consequently, the initial node, Ω_0 is determined for any day in 1965 from Figure 13 for any launch hour consistent with the restraint that the spin axis-sun angle be $30 < \lambda < 150$. The next three figures (Figures 14 through 16) have the apogee-sun angle, α plotted versus time as a family of curves defined by Ω_0. For example, consider an injection time of May 10, 1965 at 1230 hours U.T. From Figure 13 the value of the $\Omega_0 = 210°$. Then from Figure 15 the initial angle of the apogee-sun angle, α is defined as $122^{\circ}.5$ and decreasing. The time history of the curve is therefore also given by this technique because α as a function of time will follow the curve defined by Ω_0.

Since it is desired to have the initial value of $\alpha \leq 90°$ and decreasing it can be seen that the launch window is further reduced by this restraint. During May 1965 the only acceptable initial nodes (from Figure 13) are approximately between 135° and 195° which means launch should occur between 0800 U.T. and 1200 U.T. for May 1 and changing linearly to between 0600 U.T. to 1000 U.T. for May 31.

It is necessary to point out that these cross plots of Ω_0 and α are based on the assumption that the apogee vector is fixed in inertial space. In reality the apogee vector has a motion which is determined by the motion of orbital plane in space, specifically the variations of inclination, the motion of perigee and node. The analytical expression for the angle, α can be written as:

$$\alpha = \cos^{-1} [\overline{1}_p \cdot -\overline{1}_s] \tag{4}$$

where $\overline{1}_p$ = the unit vector to the perigee point from the center of the earth

$\overline{1}_s$ = the unit vector to the sun from the center of the earth.

These are shown on Sketch No. 2 in Section II-C.

$$\overline{1}_p = (x_p, y_p, z_p)$$

$$\overline{1}_s = (x_s, y_s, z_s)$$

Hence

$$\begin{aligned} x_p &= \cos\omega \cos\Omega \\ y_p &= \cos\omega \sin\Omega \\ z_p &= \sin\omega \sin i \end{aligned} \tag{5}$$

$$x_s = \cos \delta \cos RA$$
$$y_s = \cos \delta \sin RA$$
$$z_s = \sin \delta \tag{6}$$

where Ω = right ascension of the ascending node.

ω = argument of perigee.

i = inclination

RA = right ascension of the sun.

δ = declination of the sun.

Rewriting equation shows that

$$\alpha = \cos^{-1} [\cos \omega \cos \Omega \cos \delta \cos RA + \cos \omega \sin \Omega \cos \delta$$
$$\sin RA + \sin \omega \sin i \sin \delta] \tag{7}$$

Clearly from the above

$$\alpha = \alpha(\omega, \Omega, \delta, RA, t).$$

Consequently, in order to accurately define the α history computer runs are necessary using as input the most probable launch times. For planning purposes, however, the curves shown on Figures 13 through 16 are adequate.

V. ORBITAL DATA

A. Perigee Height

Perigee height curves are shown on Figures 17 through 23 for May 1965. Computer runs were made at two-hour intervals consistent with the nominal 120K n.m. launch window (see Figure 5). On all of these curves it can be seen that the mean value of perigee height is increasing in what appears to be a linear fashion. This general increasing trend is due to the combined gravitational effects of the moon, sun and the asphericity of the earth. The high frequency perturbation (approximately 14 days) is due to the periodic effect of the moon and the 180 day periodic effect is due to the sun.

On a boundary condition case the slope of the linear trend is zero except in cases where the high frequency effect of the lunar perturbation drives the perigee height below an acceptable level. Also the launch time available is considerably affected by the fact that there are times that have the linear trend increasing, but the high frequency periodic lunar perturbations drive the perigee height down below the injection height.

These cases usually occur shortly after launch, consequently, there is no trade-off possible, that is to accept a less than one year lifetime when all other conditions are favorable.

B. Eclipse Time Per Orbit

1. Earth Shadow

Figures 24 through 30 show the amount of time that the satellite will spend in the shadow of the earth for launch times during May 1965. These results are based on computer runs made at two hour intervals consistent with the nominal 120K n.m. launch window (see Figure 5). These computer runs were made with the Launch Window Program (discussed in Section II-B) which averages the high frequency lunar perturbation. The shadow of the earth is assumed to be a circular cylinder consequently there is no differentiation between penumbra and umbra. The orbits were computed for one year for each selected launch time. The eclipse time per orbit during the period considered varies from less than an hour to about eight hours.

The investigation eclipse time per orbit restraint is a study in which the number of days to an eclipse of 3.5 hours or greater is determined as a function of time. These results are also shown graphically on the year survey launch window map, Figure 3 and on the detailed launch window map, Figure 5. The interpretation of these results from the detailed launch window map is similar to year survey launch window map. On either launch window map the area above the eclipse restraint violation boundary line (marked with small circles) indicates that eclipses $\geq$ 3.5 hours will occur during the first year of flight. The amount of flight time in days prior to the eclipse time violation is also shown on the launch window maps.

2. Moon Shadow

In cases of high eccentricity orbits such as the one being considered in this analysis the problem of time spent in moon shadow is also a factor to be considered.

About the only time in the life of a satellite when moon shadow would be a problem is when the satellite passes from earth shadow into moon shadow, or vice versa. Such situations arise only prior to and after solar eclipses. For the first year of flight for the IMP-C the solar eclipses occur on the following dates (assuming a May 1965 launch):

May 30, 1965

November 23, 1965

May 20, 1966

In a worst-case situation assume that IMP-C is almost stationary in space (i.e. at apogee) then the maximum time the spacecraft could spend in the lunar shadow is approximately the amount of time it takes for the moon to travel its own diameter. This assumes a circular cylindrical lunar shadow which is also a conservative assumption.

The speed of the moon with respect to the earth is:

$$v = \sqrt{\frac{\mu}{a}} \tag{8}$$

where v = lunar speed.

μ = gravitational constant for earth.

a = semi-major axis of lunar orbit.

The use of equation (8) assumes $e = 0$ for the moon's orbit. Hence, $v =$ 1.0183 km/sec. The lunar diameter is 3476.18 km, consequently the time for the moon to travel its own diameter is 0.9483 hours.

The lunar shadow problem for IMP-C does not exist because none of the solar eclipses occur on days when the satellite will be sensing earth shadows such that the sum of the duration of the time spent in moon shadow and the time spent in the earth shadow exceeds 3.5 hours. This is assuming the worst case lunar shadow line of 0.9483 hours.

Table IV shows the maximum possible amount of times that can be spent in combined earth and moon shadow for launch times during May 1965.

Table IV
Earth and Moon Shadow Time

Launch Date	Flight Time to Solar Eclipse in Days	Time in Earth Shadow on Day of Eclipse in Hours	Maximum Possible Time in Moon Shadow in Hours	Total Possible Time in Eclipse in Hours
FOR ECLIPSE OF MAY 30, 1965				
May 1	29	0.0000	0.9483	0.9483
May 6	24	0.1800	0.9483	1.1283
May 11	19	0.0000	0.9483	0.9483
May 16	14	0.0000	0.9483	0.9483
May 21	9	0.0000	0.9483	0.9483
May 26	4	0.0000	0.9483	0.9483
May 31	0	0.0000	0.9483	0.9483
			0.9483	0.9483
FOR ECLIPSE OF NOVEMBER 23, 1965				
May 1	206	0.4000	0.9483	1.3483
May 6	201	0.3600	0.9483	1.3083
May 11	196	0.3000	0.9483	1.2483
May 16	191	0.3800	0.9483	1.3283
May 21	186	0.3500	0.9483	1.2983
May 26	181	0.4000	0.9483	1.3483
May 31	176	0.3900	0.9483	1.3383
FOR ECLIPSE OF MAY 20, 1966				
May 1	-	-	-	-
May 6	-	-	-	-
May 11	-	-	-	-
May 16	-	-	-	-
May 21	364	0.0000	0.9483	0.9483
May 26	359	0.0000	0.9483	0.9483
May 31	354	1.2500	0.9483	2.1983

C. Inclination

Figures 31 and 32 show the behavior of inclination for four different launch times with respect to time (for one year of flight). The computations for these results were done with the Launch Window Program consequently the high frequency lunar perturbation is not apparent. Its effect is averaged. On all four of the launch times shown on Figures 31 and 32 the inclination is seen to have a mean increasing trend. The 180 day periodic effect is due to the solar perturbation. There is a relationship between the change in perigee height as a function of time and the change in inclination such that increases in perigee height and increases in the average slope of inclination occur at the same time.

D. Declination of Apogee

The declination δ_a of apogee is defined in the sketch below:

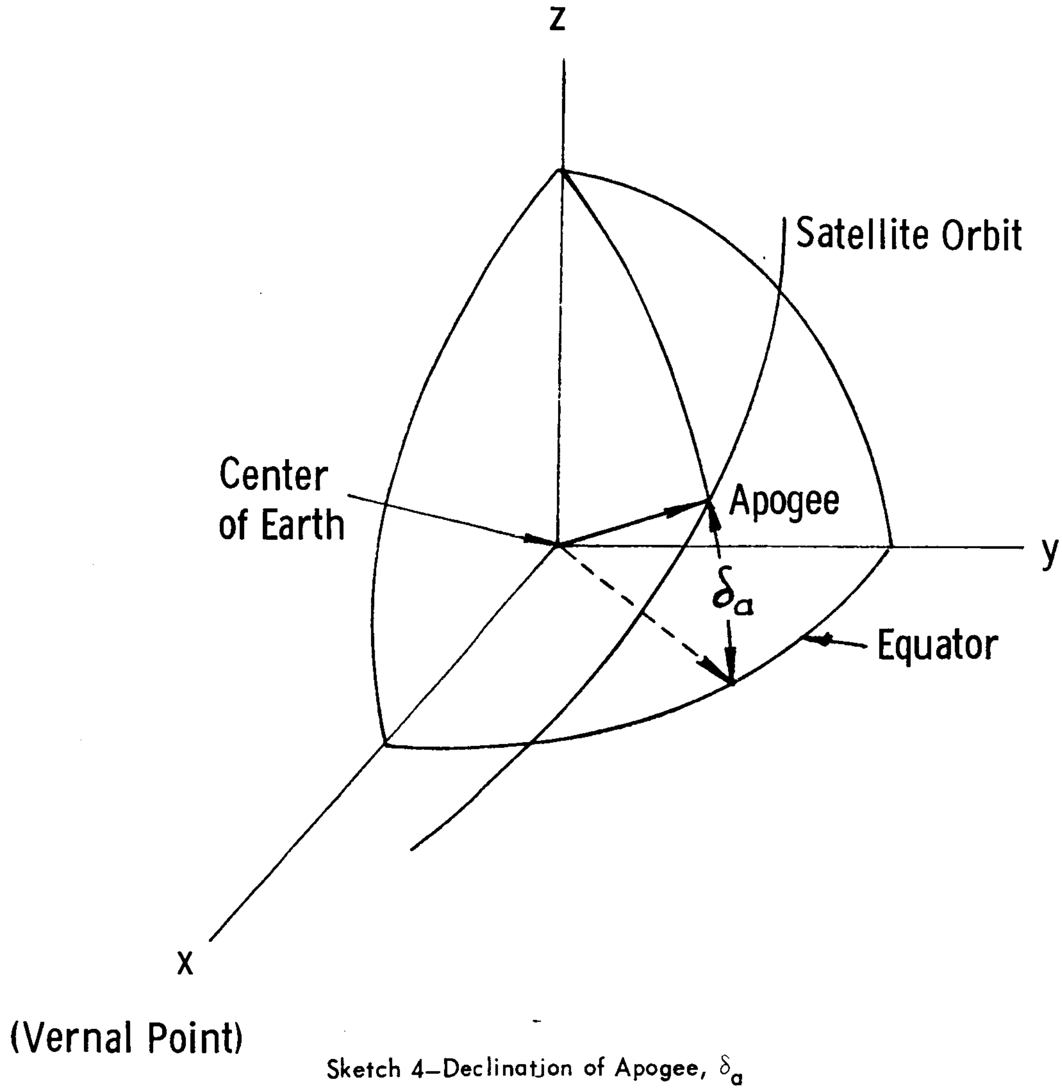

Sketch 4—Declination of Apogee, δ_a

On Figures 33 and 34 the behavior of declination of apogee is shown for a year of orbital life for four different launch times. Initially for the nominal IMP-C orbit $\delta_a = -23^\circ\!.105$ and the trend is toward zero declination. When $\delta_a = 0$ occurs the apogee will be in the plane of the equator.

The declination of apogee curves were computed with the Launch Window program, hence the high frequency lunar perturbation is averaged. The 180 day periodic effect is due to the solar perturbation.

VI. CONCLUSION

The most important results of this document are summarized in Table V on the following page which shows the launch times available for May 1965 taking into consideration the two mandatory restraints, namely lifetime and spin axis-sun angle. The table is based on the use of the 120K n.m. orbit. The effects of $\pm 3\sigma$ are taken into consideration on the times shown for the lifetime window (i.e. perigee height restraint). In some cases the window is closed by the $+3\sigma$ effects where in others the -3σ effects dominate.

From the detailed launch window map (Figure 5) it can be seen that there are days when there are as many as three distinct time periods on some days during which the lifetime restraint is satisfied. However, for any day there is only one time period available which satisfies the spin axis-sun angle, λ restraint.

Table V
Launch Window Table for May 1965

	LIFETIME 30 CONSERVATIVE						SPIN AXIS-SUN ANGLE $30° \leq \lambda \leq 150°$	$45° \leq \lambda \leq 135°$		
	OPEN	CLOSED	OPEN	CLOSED	OPEN	CLOSED	OPEN	OPEN	CLOSED	CLOSED
(1) MAY 1	*2157	0057	0554	1212			0500	0830	1012	1348
(2) 2	*2157	0142	0609	1215			0454	0827	1009	1345
(3) 3	*2209	0148	0618	1206			0449	0824	1006	1342
(4) 4	*2318	0054	0239	0354	0618	1142	0446	0818	1000	1338
(5) 5	0257	1109					0442	0818	0957	1334
(6) 6	0312	1027					0439	0812	0952	1330
(7) 7	0328	0948					0436	0809	0948	1326
(8) 8	0342	0936					0430	0806	0944	1322
(9) 9	0400	0939					0426	0800	0940	1318
(10) 10	0418	0951					0424	0757	0936	1314
(11) 11	0436	1009					0418	0754	0934	1310
(12) 12	*2139	*2236	0450	1034			0415	0748	0930	1306
(13) 13	*2142	*2314	0506	1054			0412	0744	0924	1302
(14) 14	*2142	*2354	0521	1114			0408	0742	0921	1257
(15) 15	*2142	0034	0536	1112			0404	0736	0918	1252
(16) 16	*2144	0112	0551	1107			0400	0734	0912	1248
(17) 17	*2145	0157	0602	1107			0354	0730	0909	1244
(18) 18	*2206	0254	0609	1105			0352	0724	0903	1240
(19) 19	*2318	0418	0603	1045			0348	0722	0900	1236
(20) 20	0121	1012					0344	0718	0954	1232
(21) 21	0212	0926					0340	0715	0852	1228
(22) 22	0236	0909					0336	0712	0848	1224
(23) 23	0309	0909					0332	0708	0842	1220
(24) 24	0330	0921					0328	0703	0839	1216
(25) 25	0354	0936					0324	0700	0836	1212
(26) 26	*2124	*2206	0414	1000			0320	0654	0830	1207
(27) 27	*2122	*2300	0436	1021			0317	0652	0827	1203
(28) 28	*2121	*2342	0454	1022			0312	0648	0822	1200
(29) 29	*2118	0018	0514	1015			0309	0642	0818	1154
(30) 30	*2118	0057	0536	1010			0306	0639	0815	1151
(31) 31	*2124	0136	0556	1006			0303	0636	0812	1148
(32)										

GSFC 6-3 (2/64)

REFERENCES

1. Shaffer, F., Squires, R. K. and Wolf, H., Interplanetary Trajectory Encke Method (ITEM) Program Manual, Document No. X-640-63-71 (Greenbelt, Maryland: Goddard Space Flight Center, May 1963).

2. Private communication with Frank Piszkin, Spacecraft Systems Branch, Goddard Space Flight Center, December 1, 1964.

3. Musen, P., A Discussion of Halphen's Method for Secular Perturbations and its Application to the Determination of Long Range Effects in the Motions of Celestial Bodies, Part I, (NASA Technical Report R-176, 1963).

4. Moe, M. M., Solar-Lunar Perturbations of the Orbits of an Earth Satellite, (American Rocket Society Journal, May 1960), pp. 485-487.

5. Smith, A. J., Jr., A Discussion of Halphen's Method for Secular Perturbations and its Application to the Determination of Long Range Effects in the Motions of Celestial Bodies, Part II, (NASA Technical Report R-194, 1964).

6. Shute, B. E., Prelaunch Analysis of High Eccentricity Orbits, (NASA Technical Note D-2530, 1964).

7. Montgomery, H. E. and Paddack, S. J., S-49, EGO Launch Window and Orbit, Document No. X-643-63-119 (Greenbelt, Maryland: Goddard Space Flight Center, July 1963).

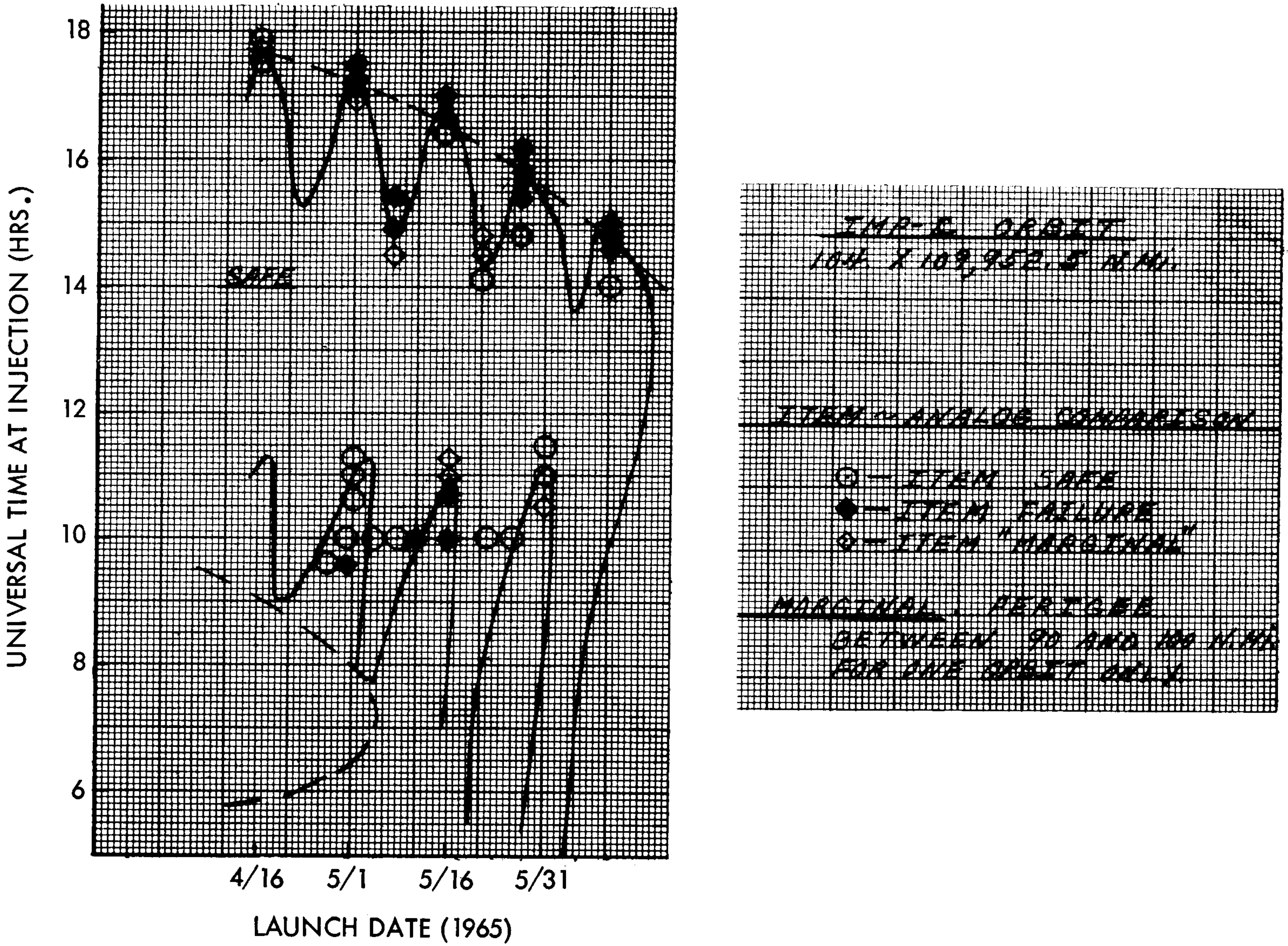

Figure 1-Program Comparison

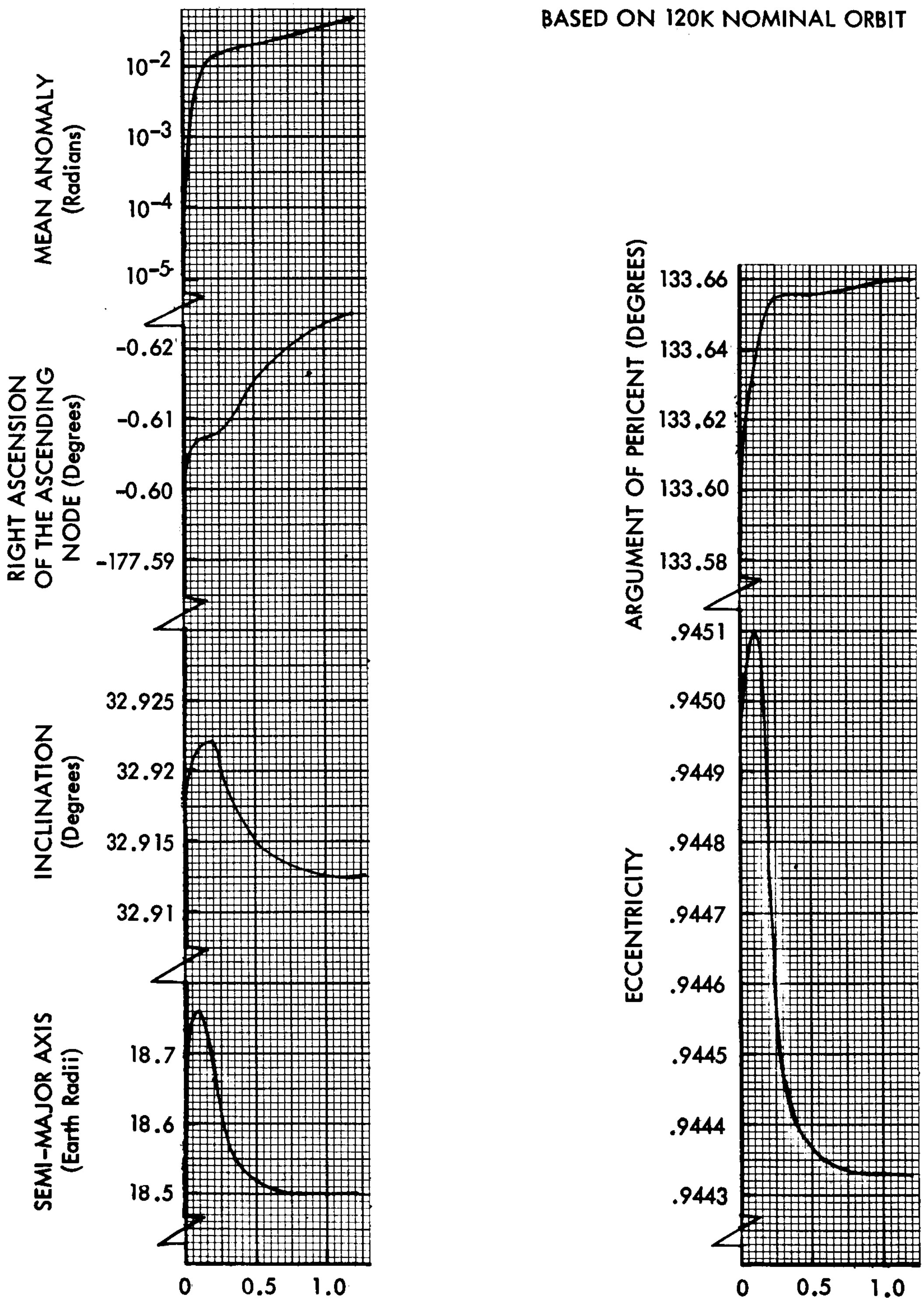

Figure 2-Orbital Elements at Perigee

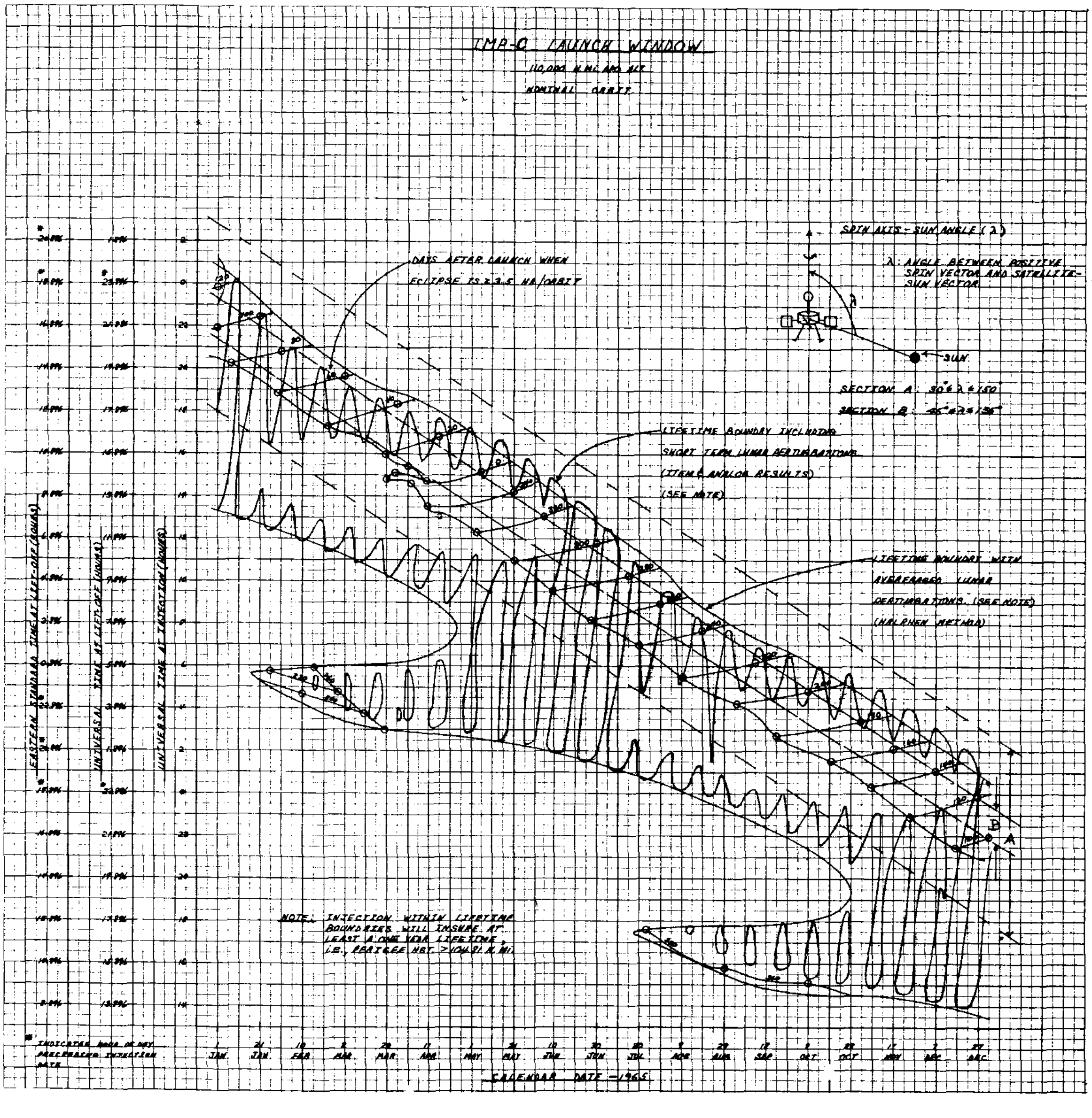

Figure 3-Launch Window Map, Year Survey (~~120K~~ 110K n.m. orbit)

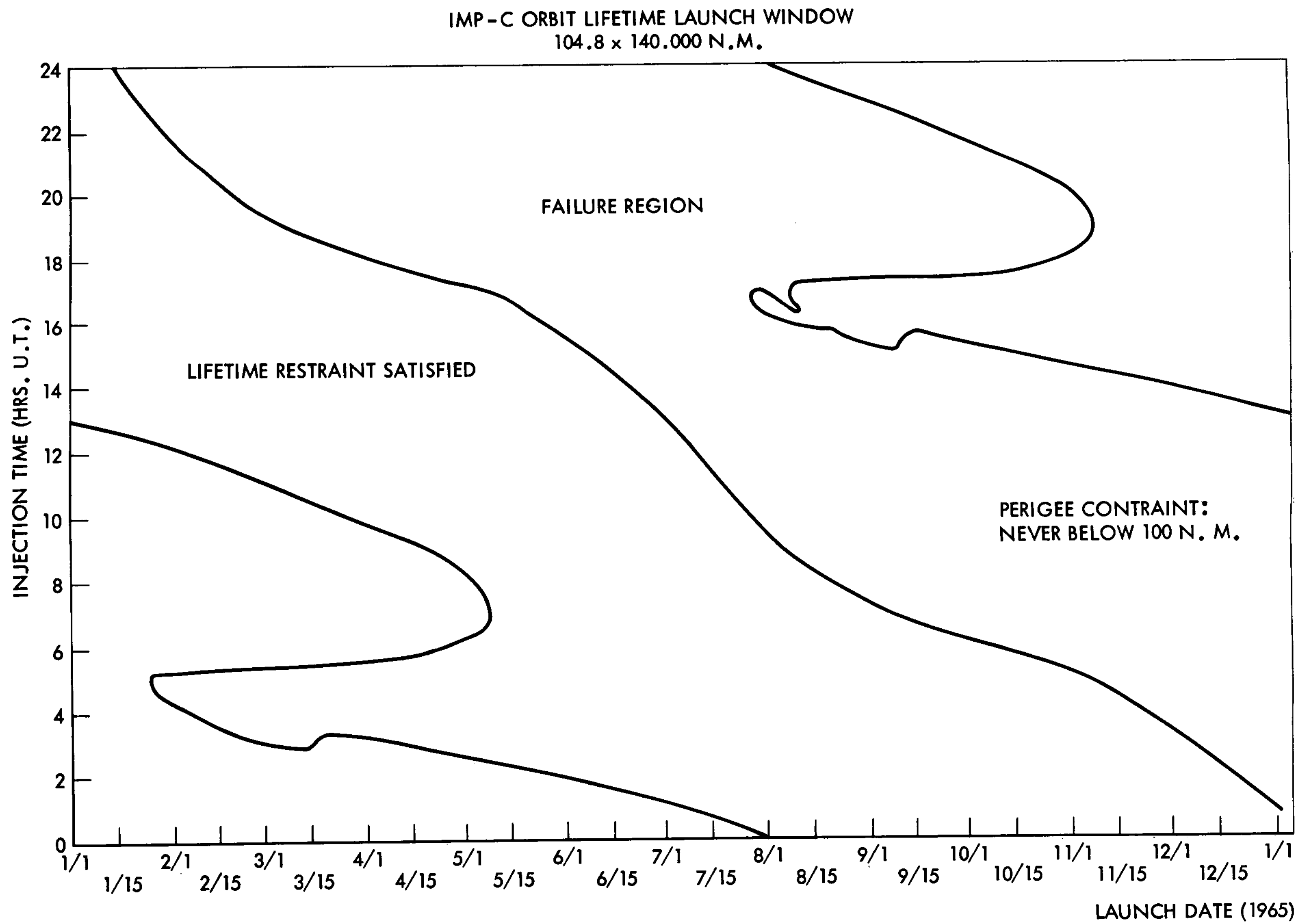

Figure 4-Launch Window Map, Year Survey (140K n.m. orbit)

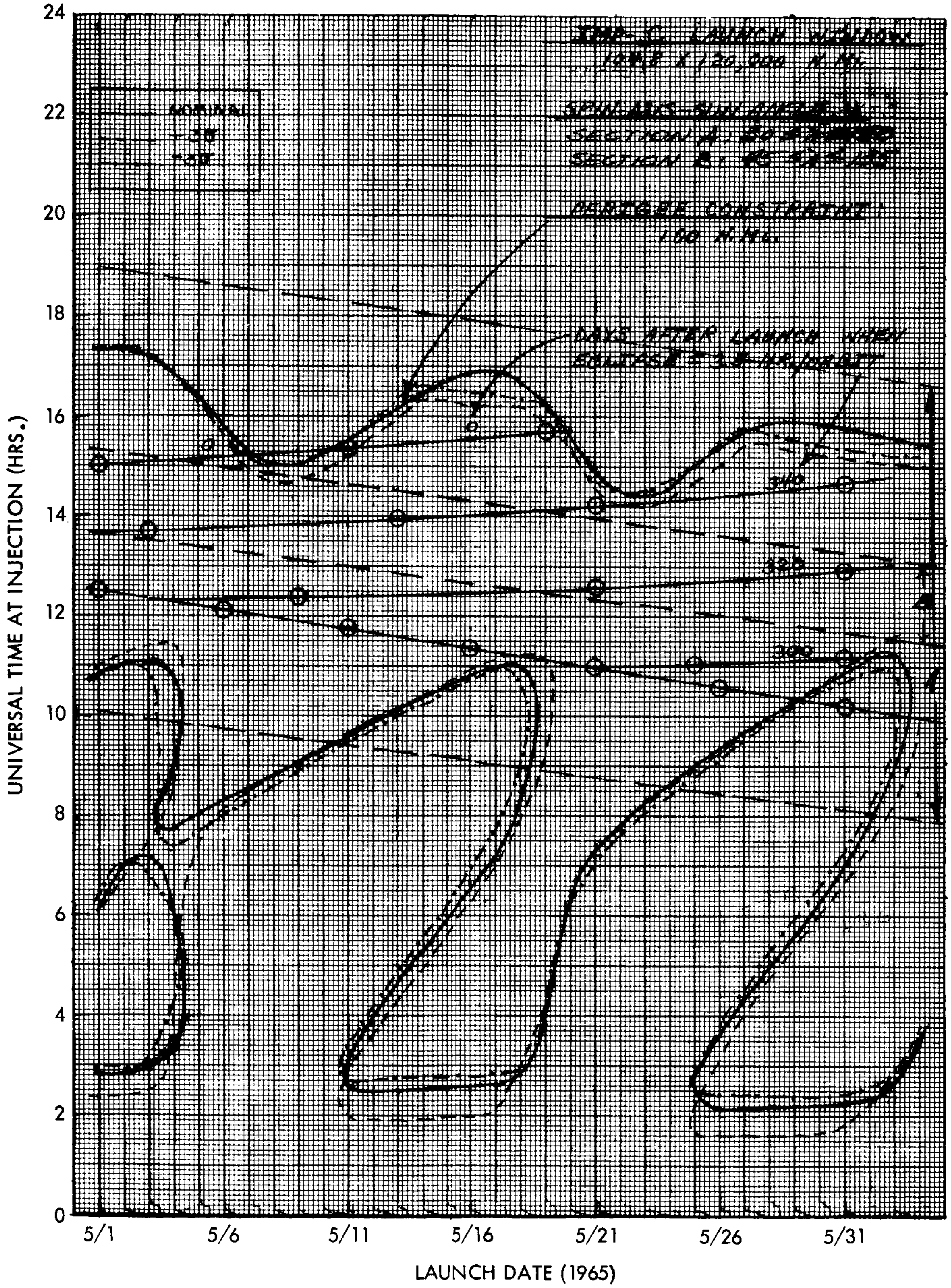

Figure 5-Detailed Launch Window, May 1965

IMP-C LAUNCH WINDOW STUDY
Apogee Altitude (N.M.) = 120,000

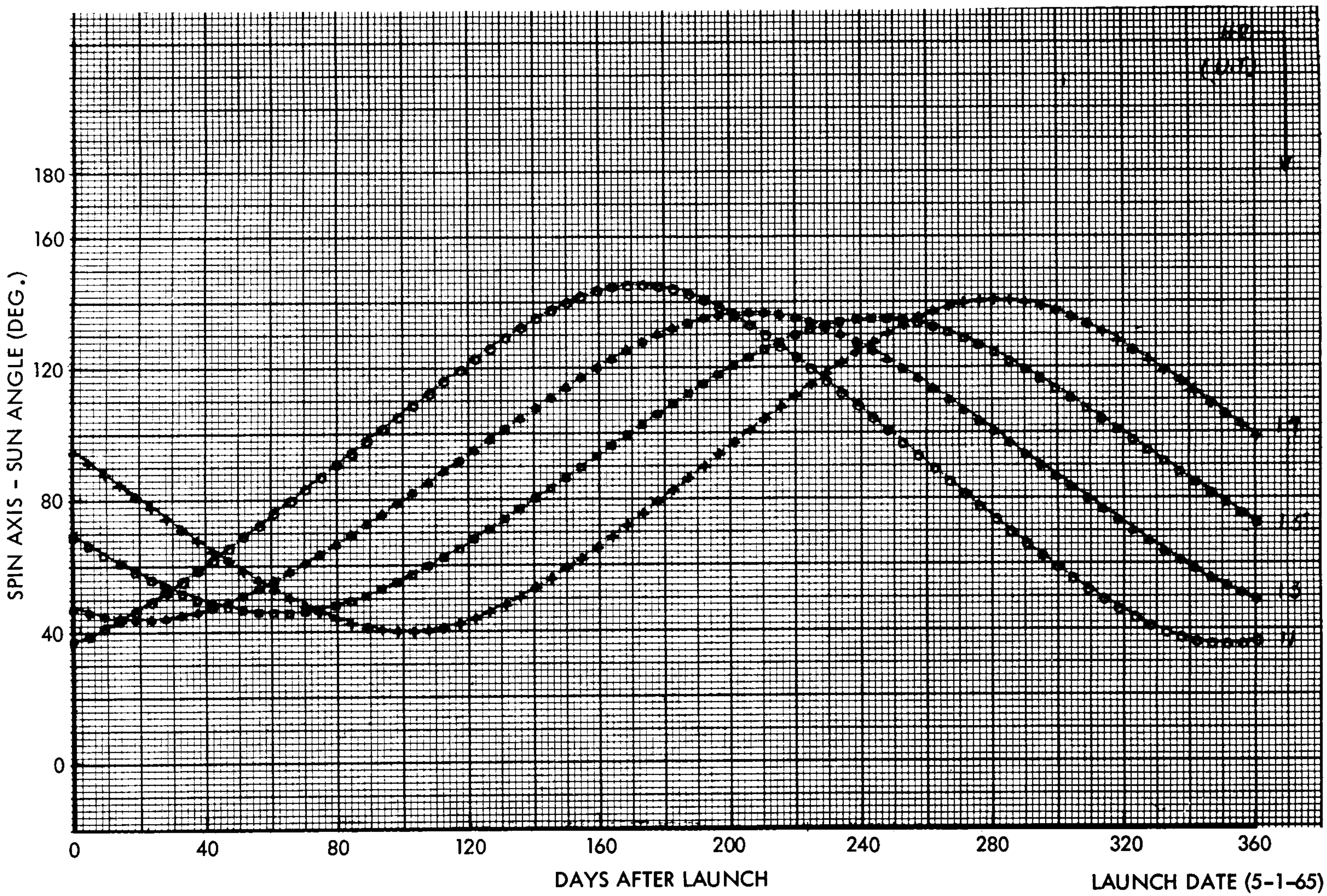

Figure 6-Spin Axis - Sun angle, λ

IMP-C LAUNCH WINDOW STUDY
Apogee Altitude (N.M.) = 120,000

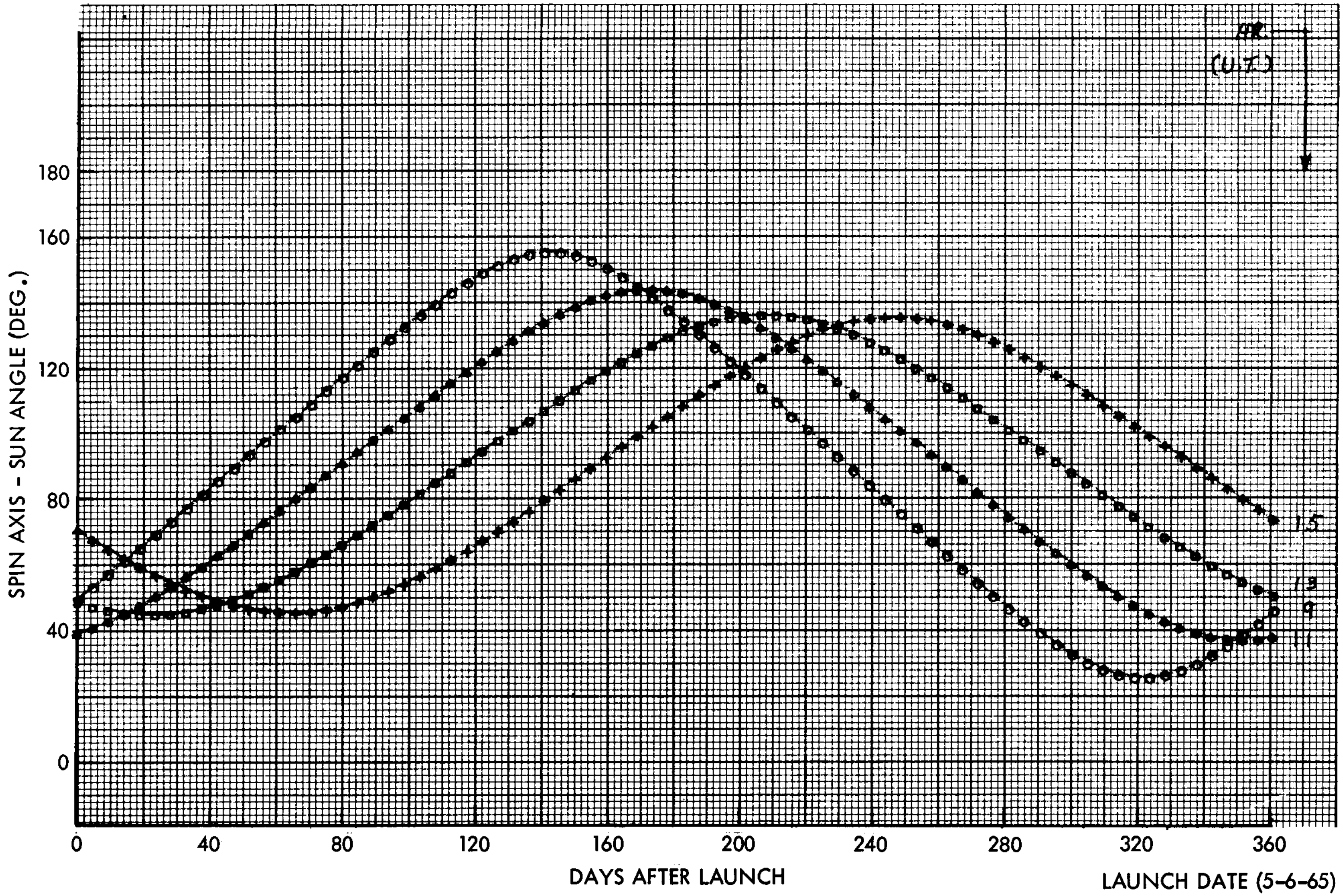

Figure 7-Spin Axis - Sun Angle, λ

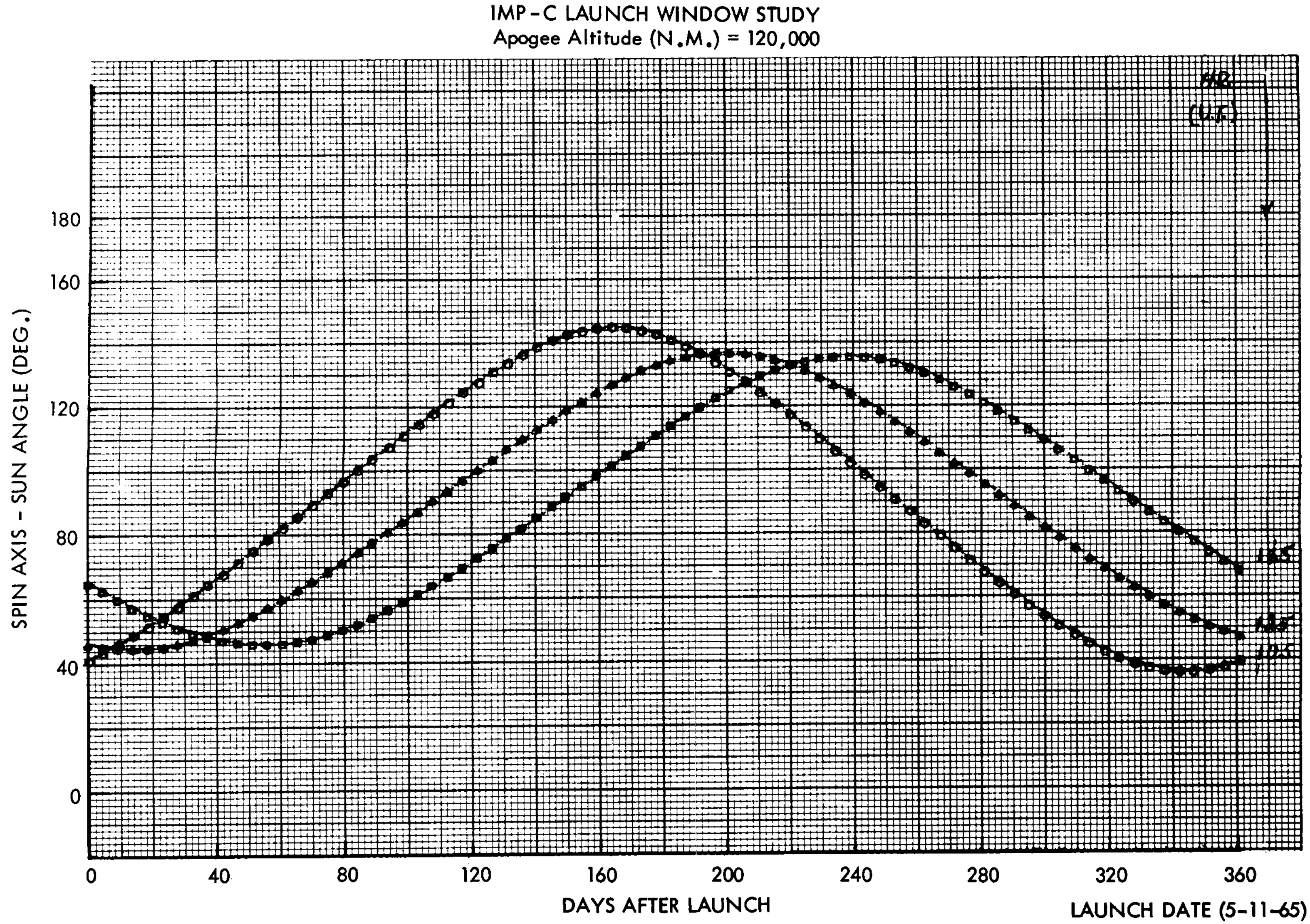

Figure 8-Spin Axis - Sun Angle, λ

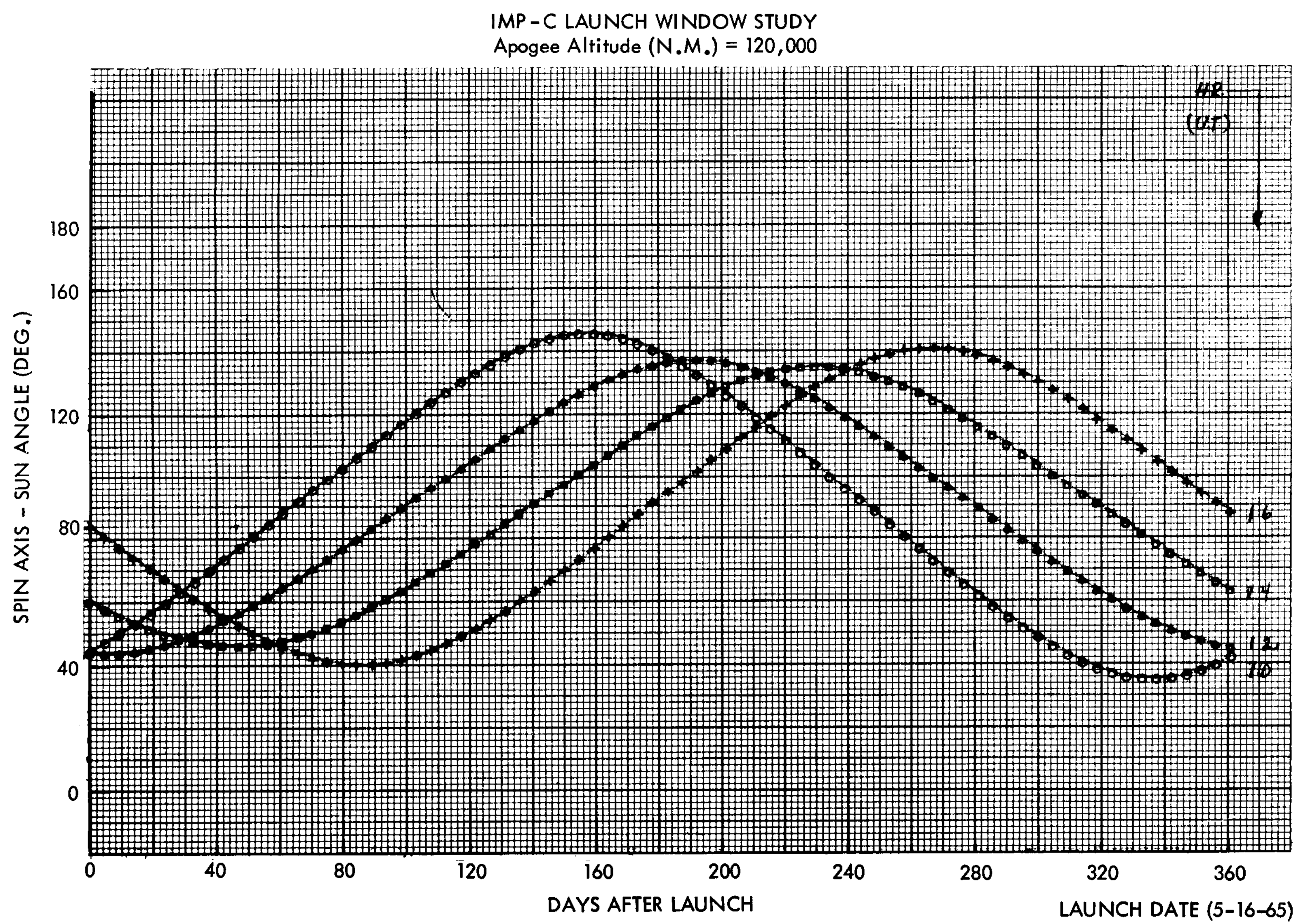

Figure 9-Sin Axis - Sun Angle, λ

IMP-C LAUNCH WINDOW STUDY
Apogee Altitude (N.M.) = 120,000

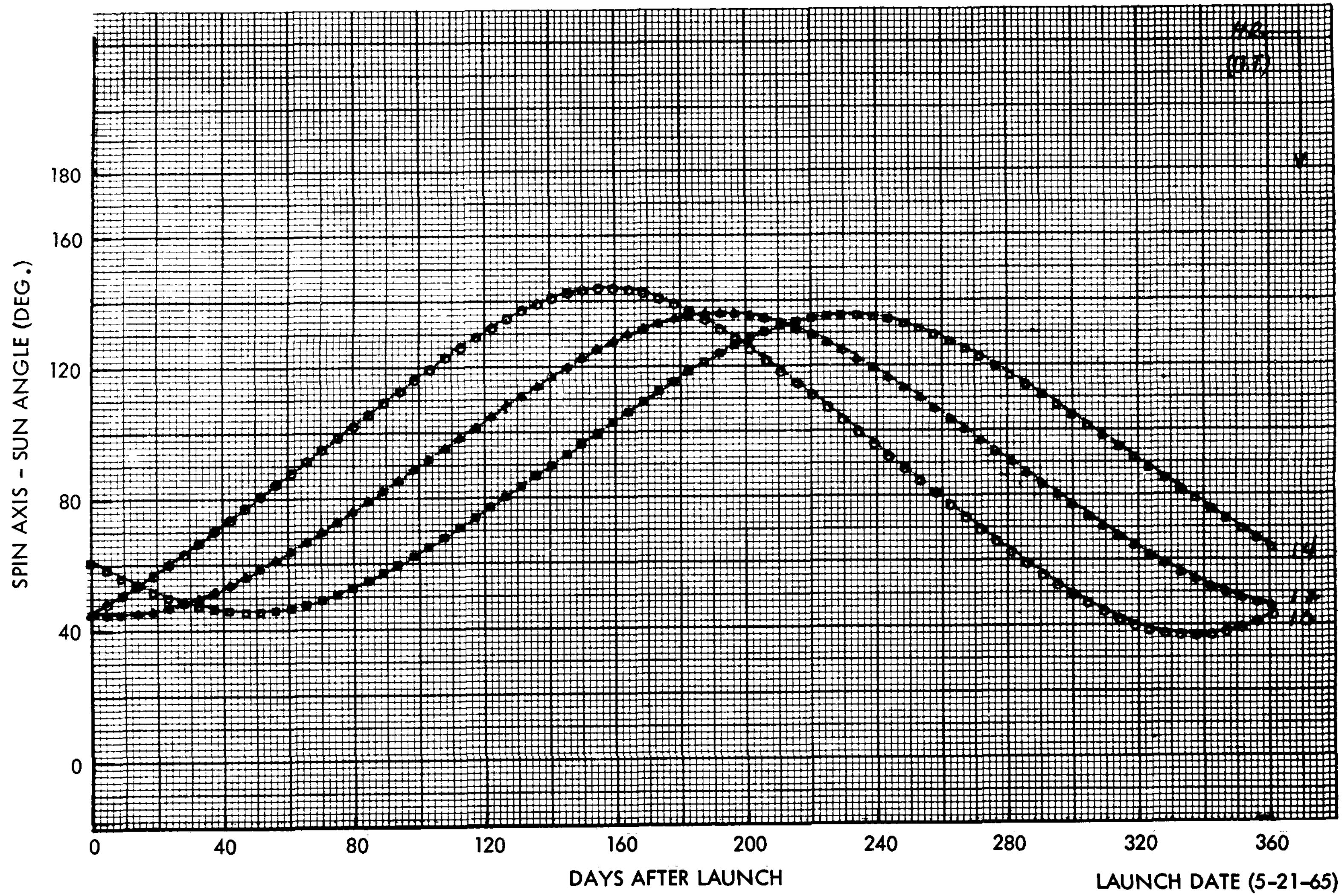

Figure 10-Spin Axis - Sun Angle, λ

IMP-C LAUNCH WINDOW STUDY
Apogee Altitude (N.M.) = 120,000

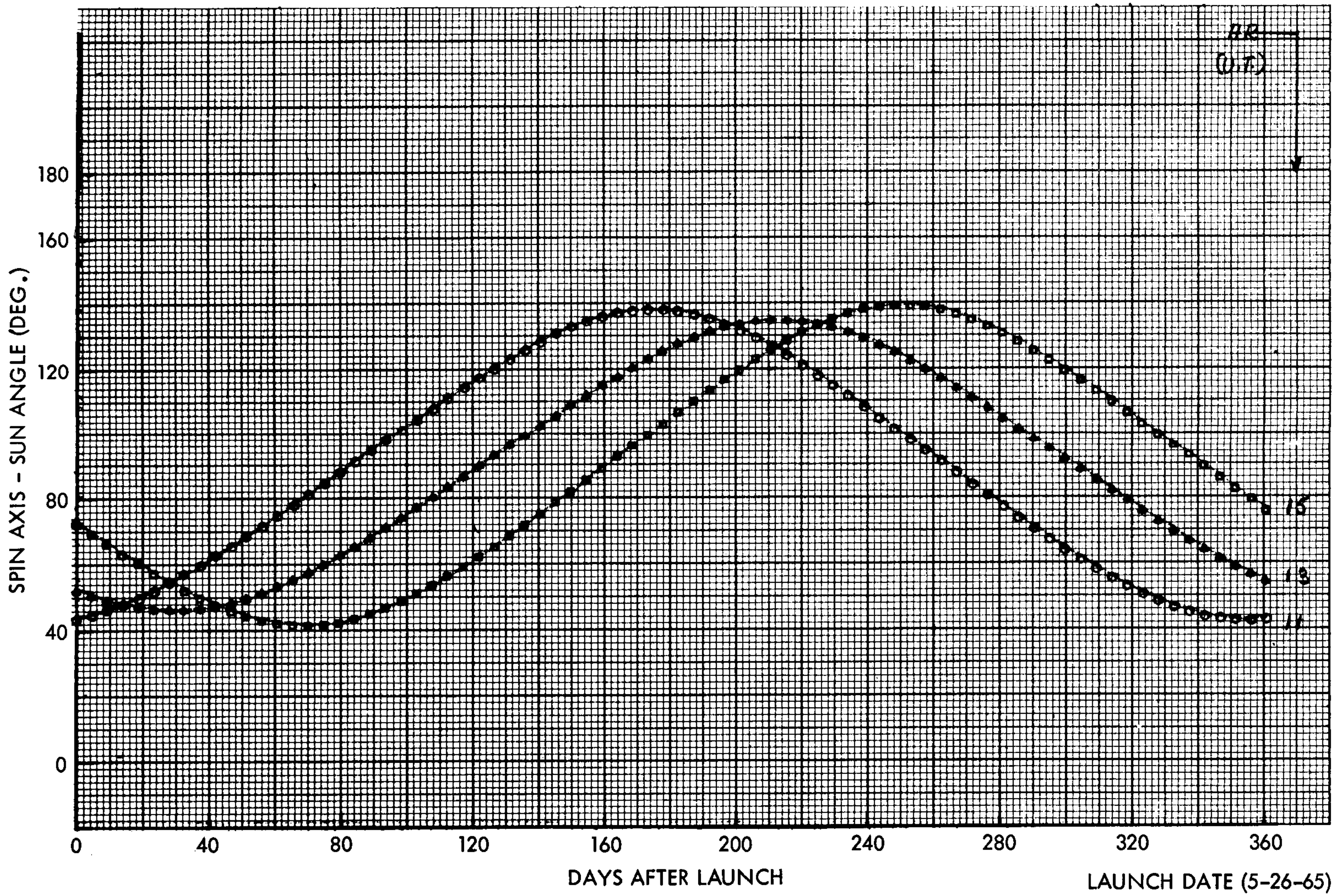

Figure 11-Spin Axis - Sun Angle, λ

IMP-C LAUNCH WINDOW STUDY
Apogee Altitude (N.M.) = 120,000

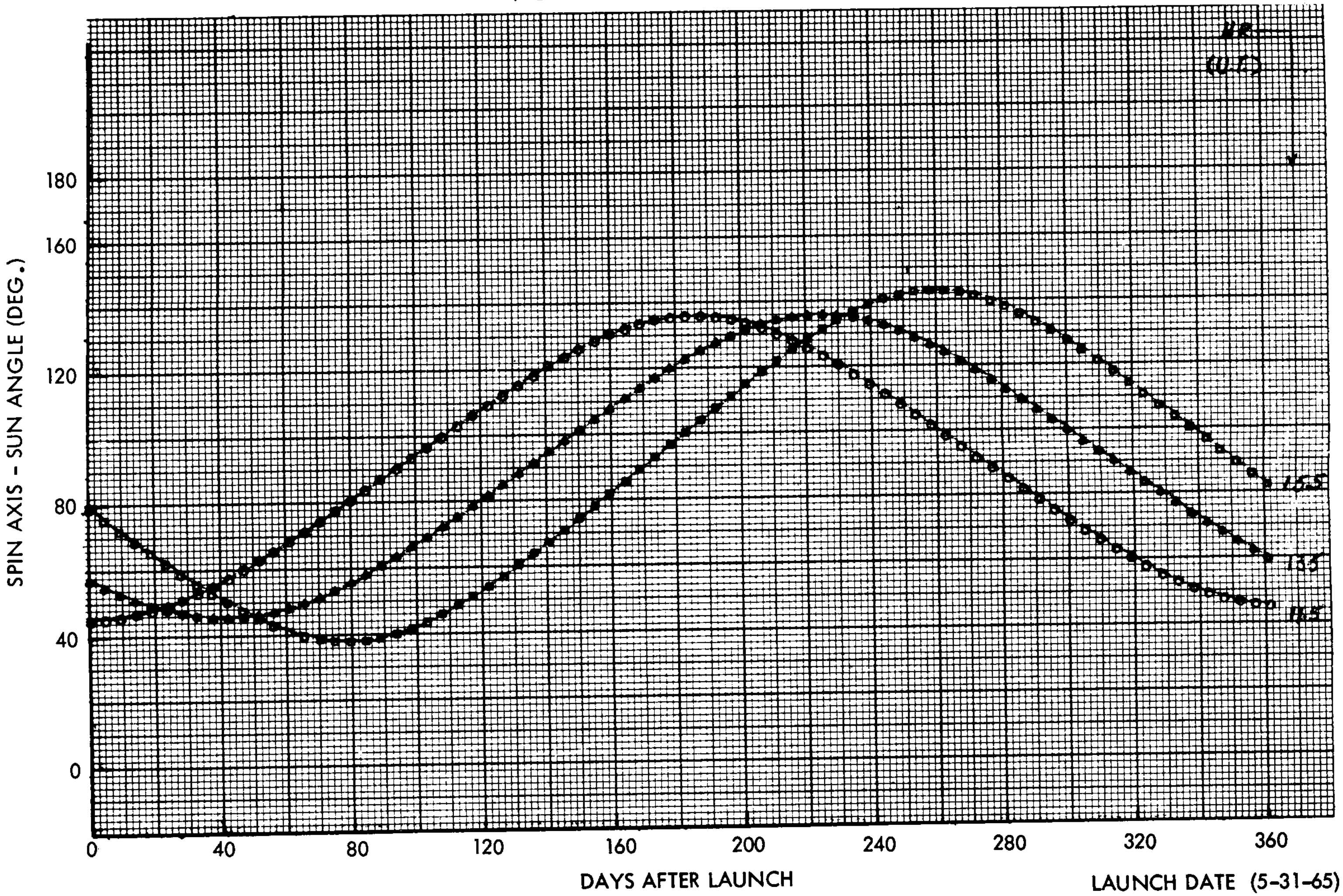

Figure 12-Spin Axis - Sun Angle, λ

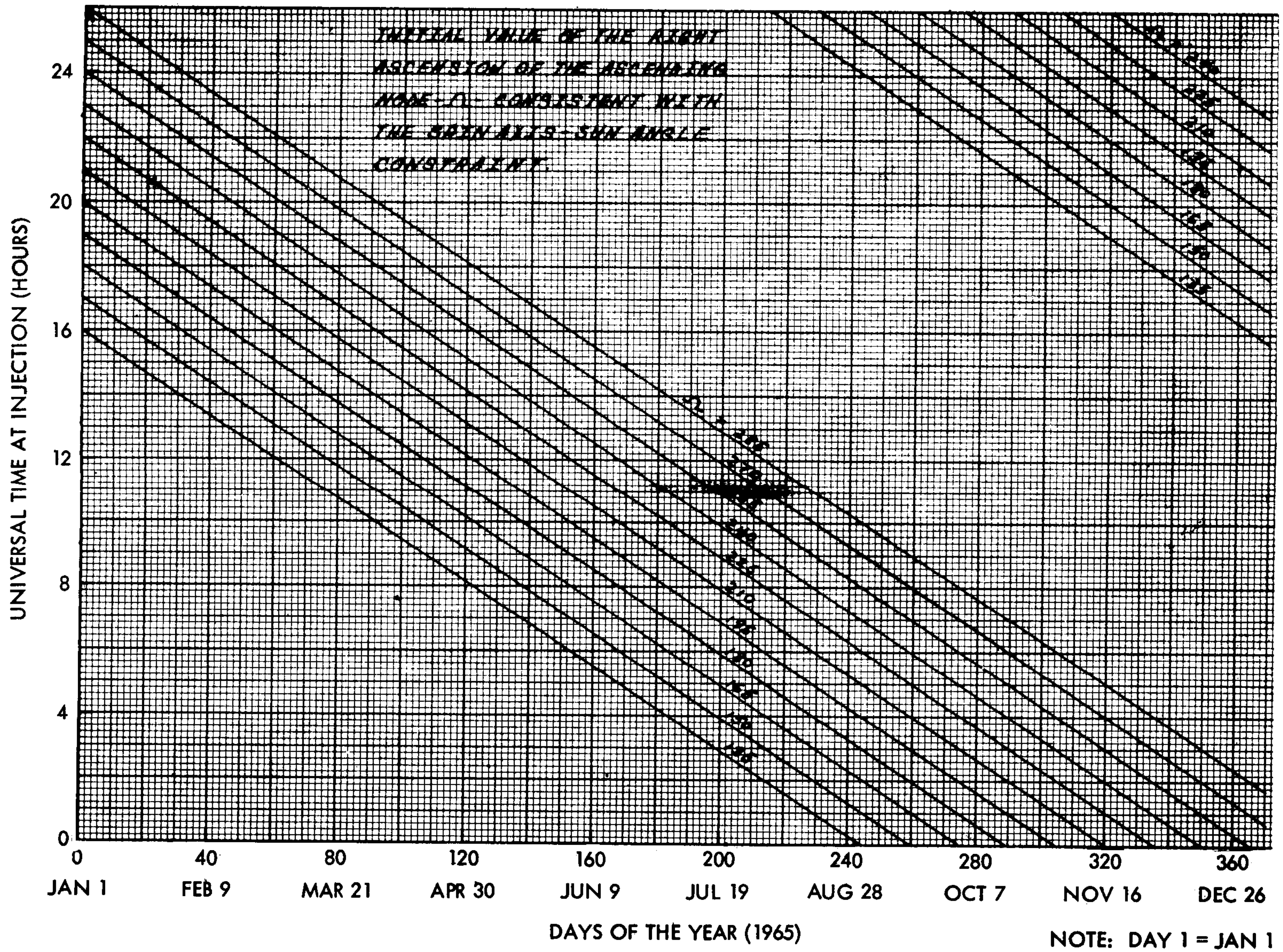

Figure 13–Initial Value of the Right Ascension of the Ascending Node, Ω_0

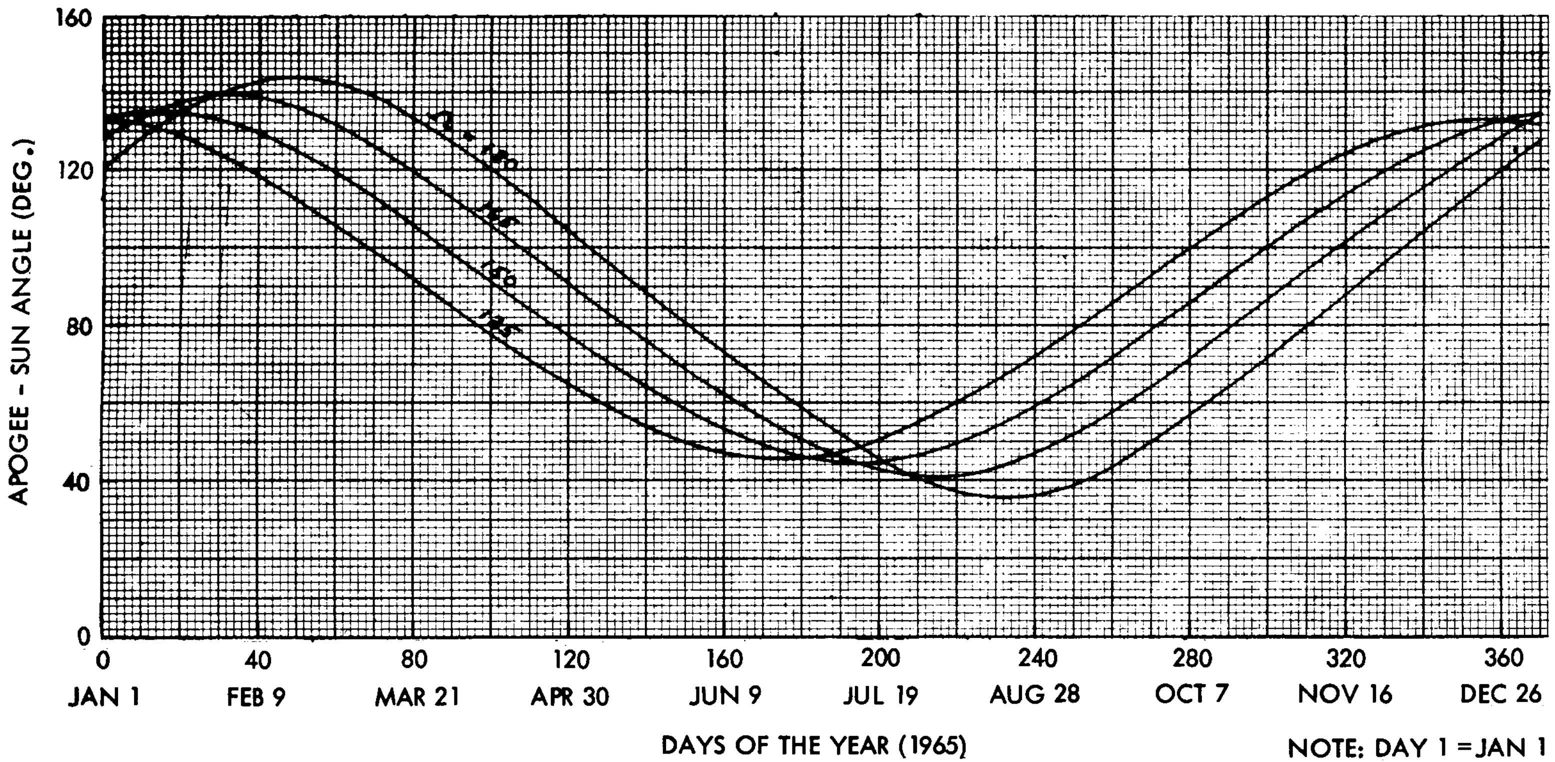

Figure 14-Apogee - Sun Angle, α

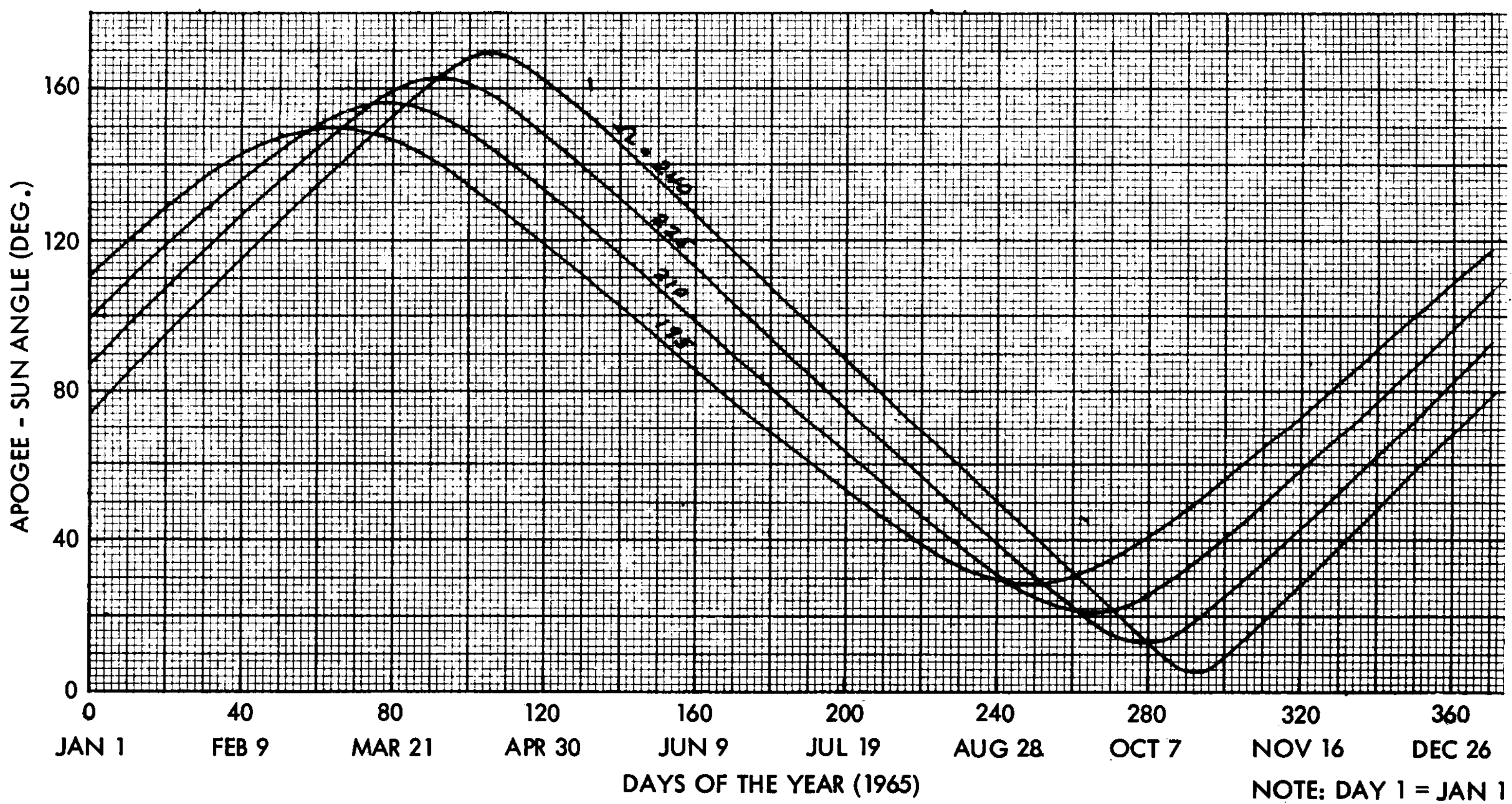

Figure 15-Apogee - Sun Angle, α

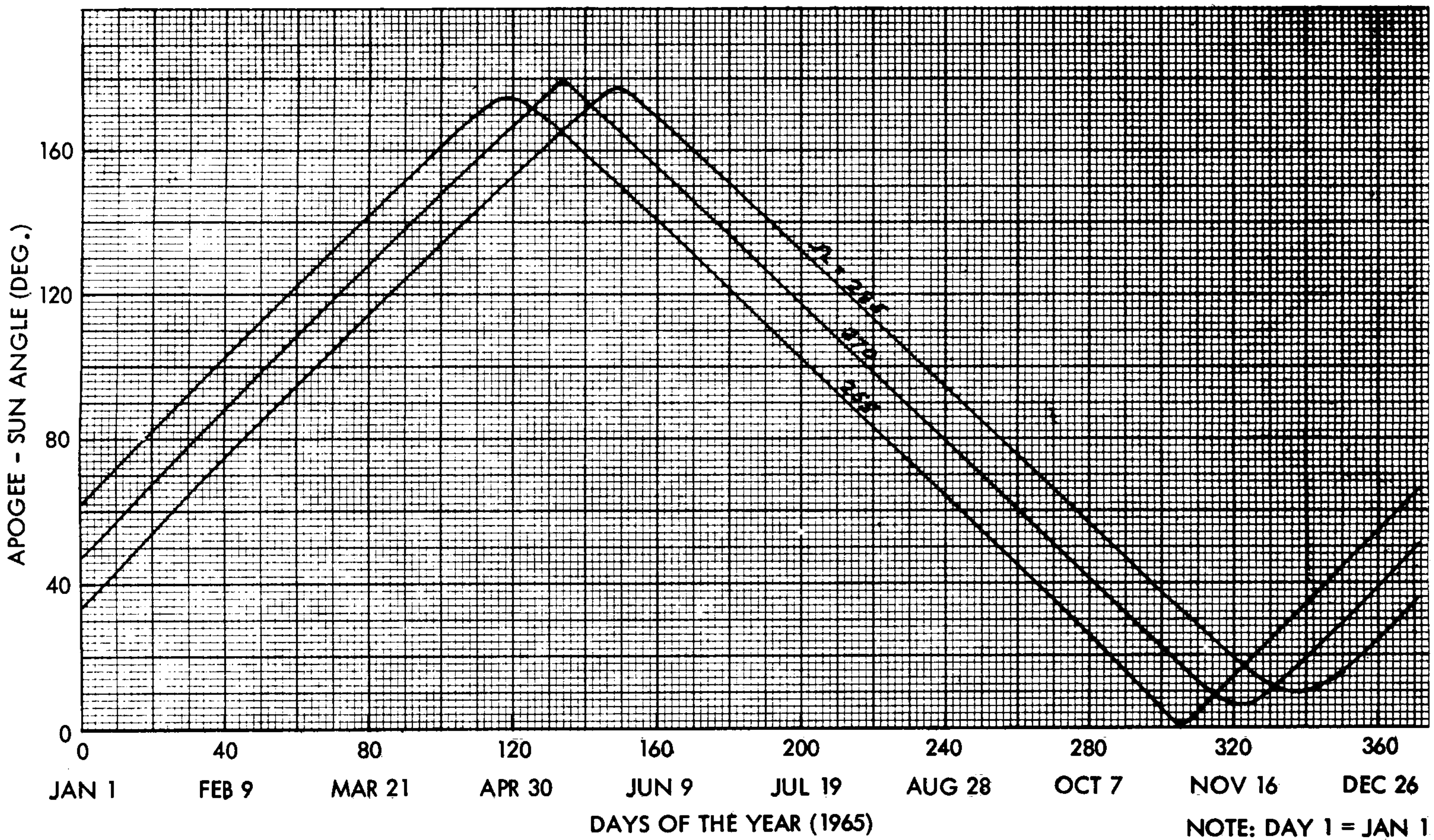

Figure 16–Apogee – Sun Angle, α

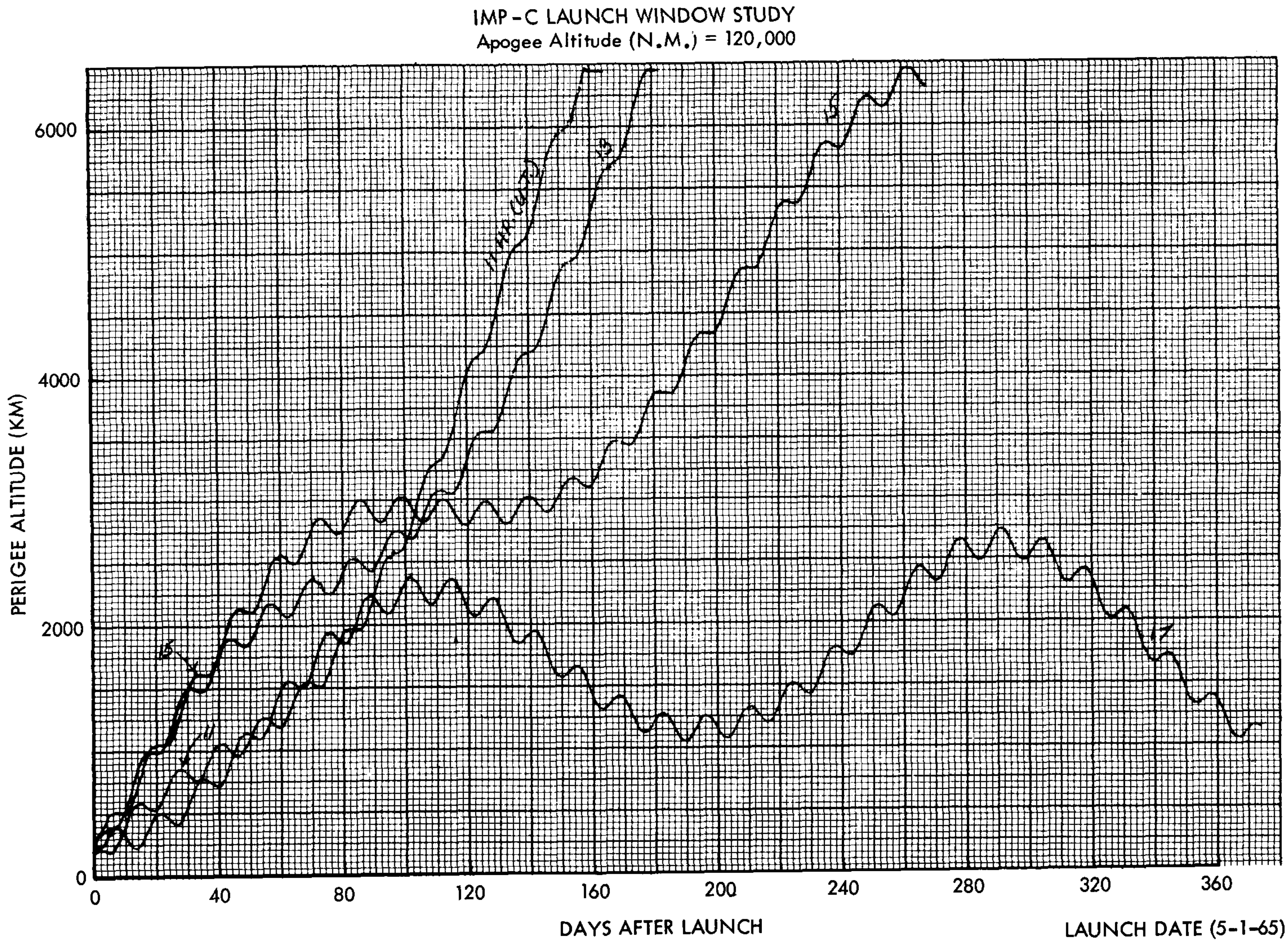

Figure 17–Perigee Height

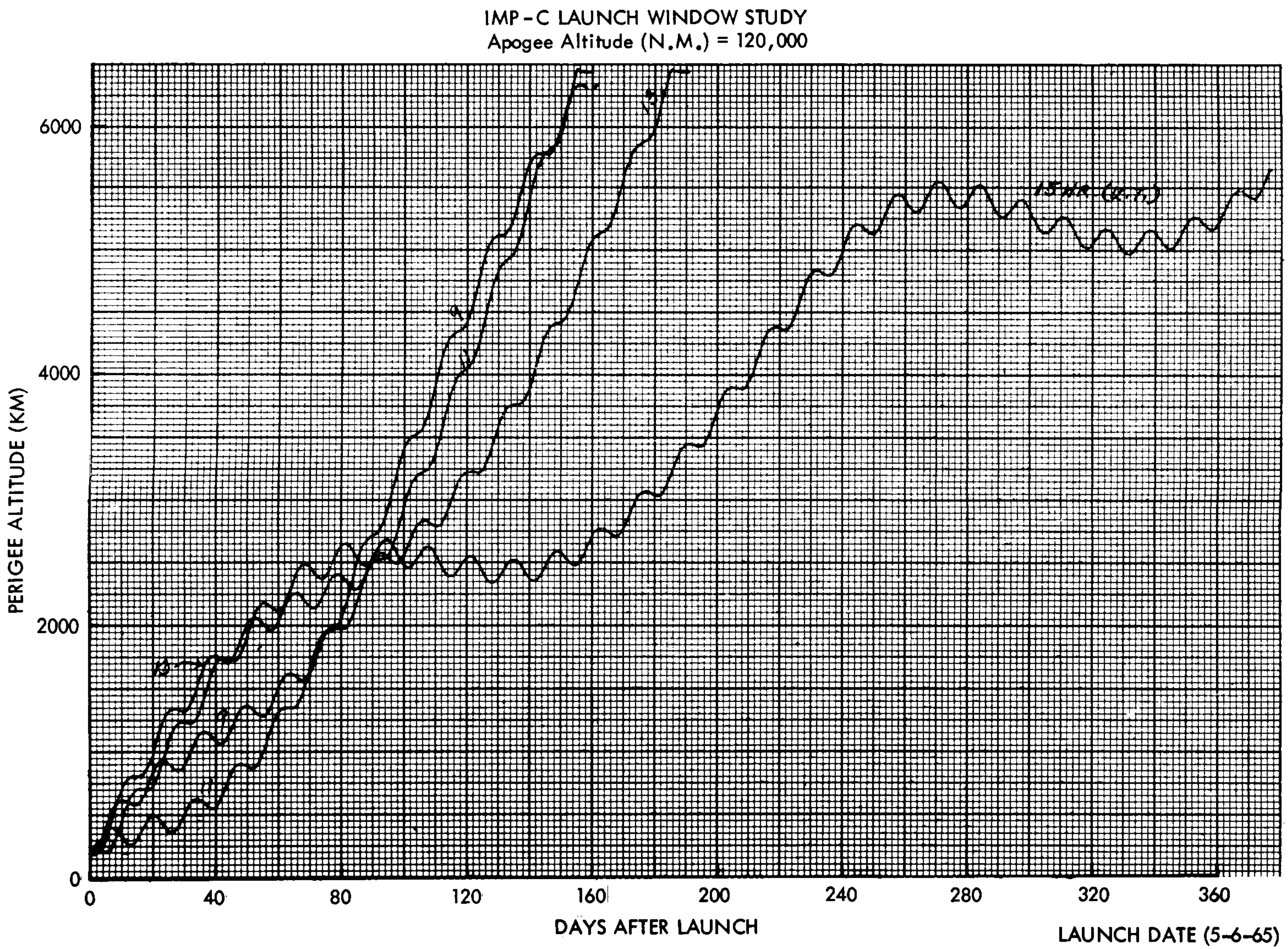

Figure 18–Perigee Height

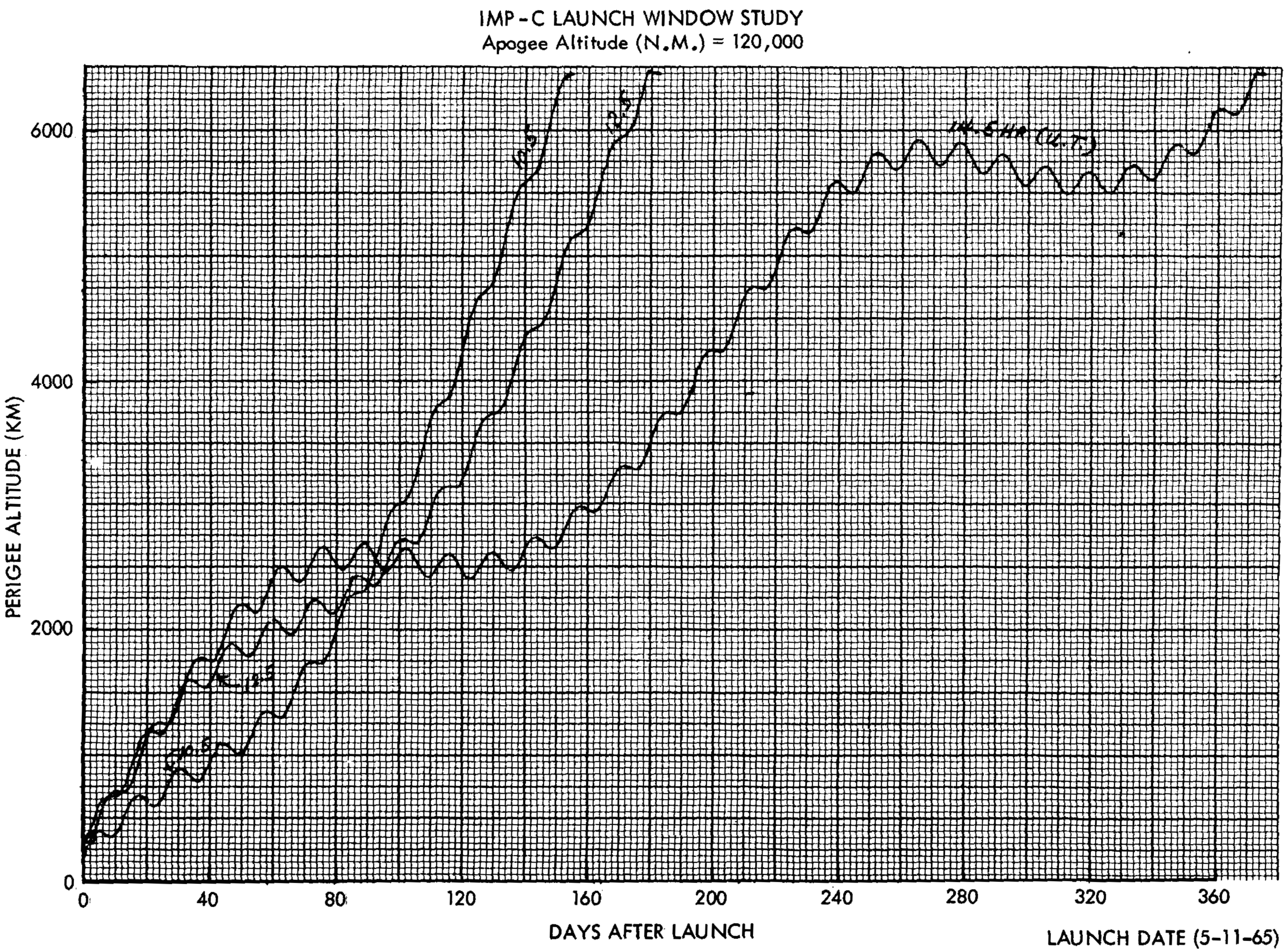

Figure 19–Perigee Height

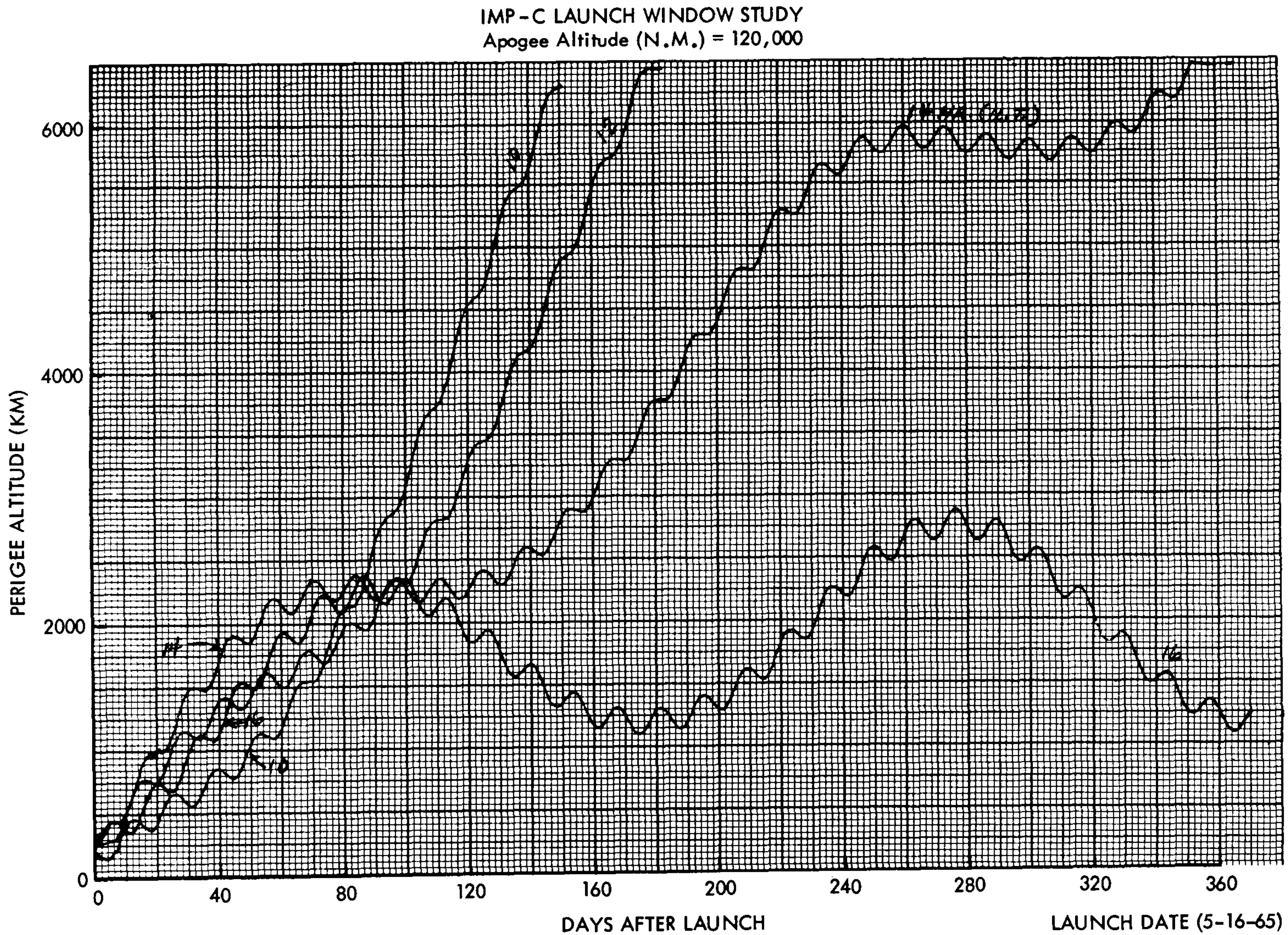

Figure 20–Perigee Height

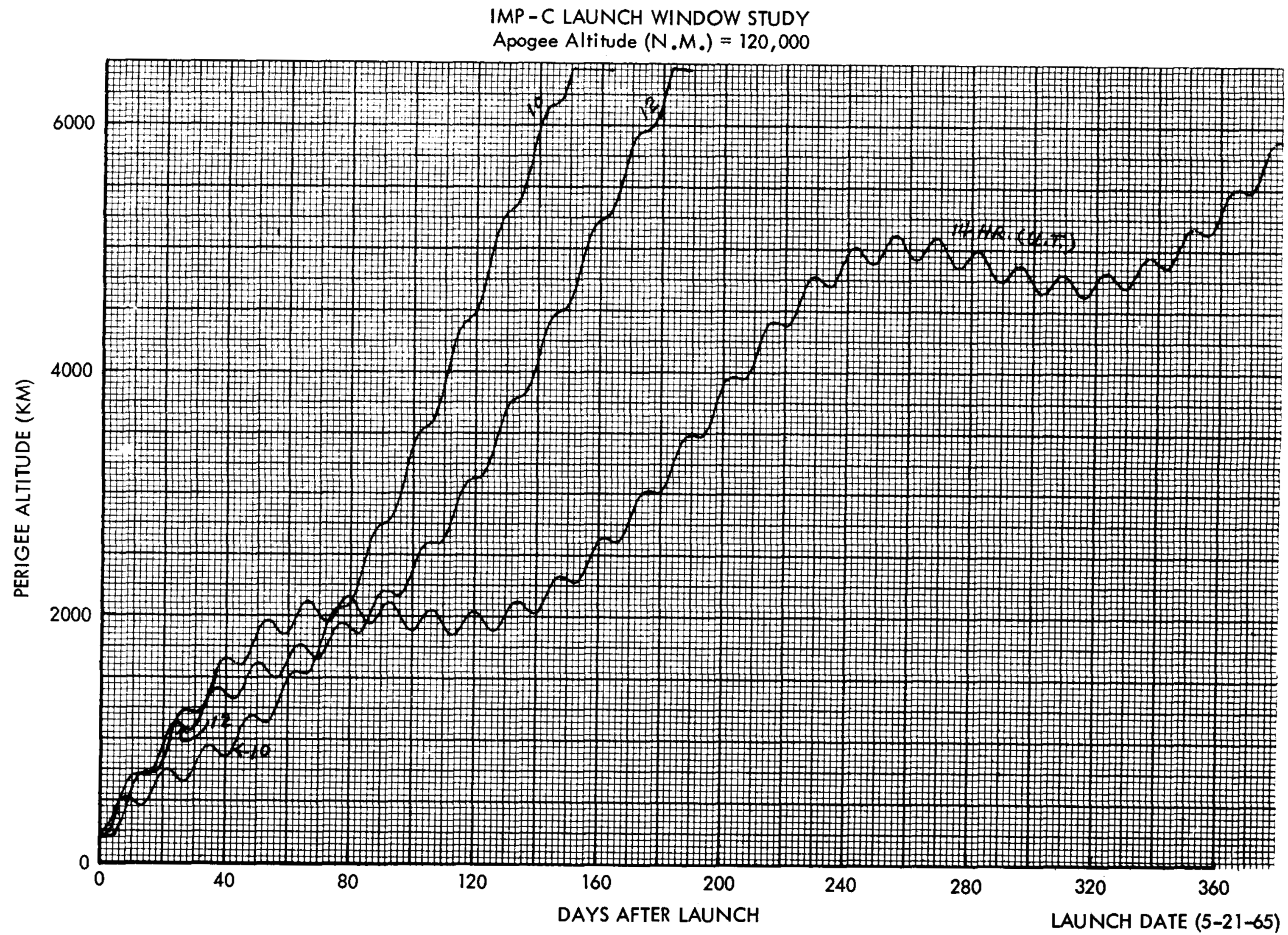

Figure 21—Perigee Height

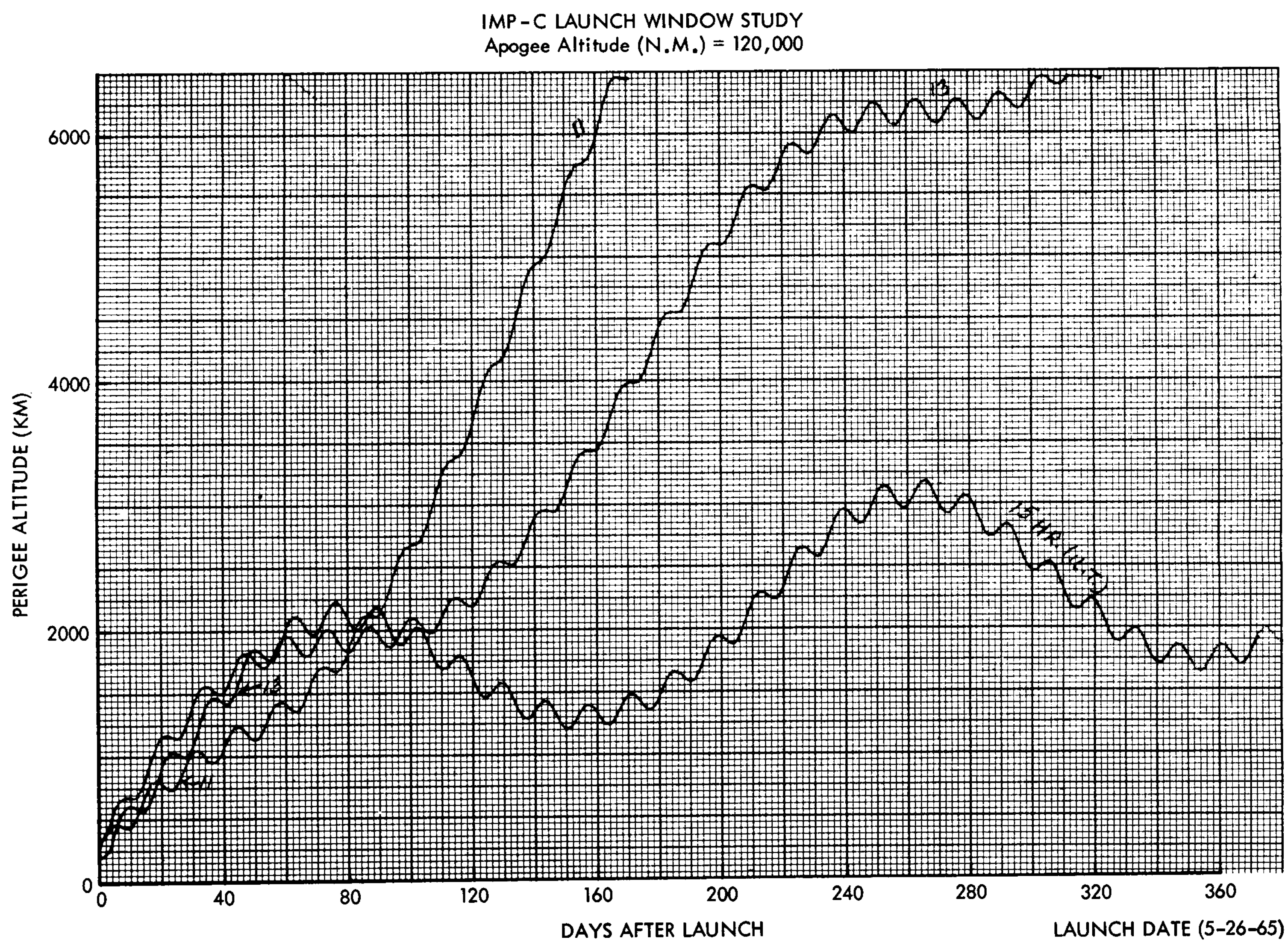

Figure 22–Perigee Height

IMP-C LAUNCH WINDOW STUDY
Apogee Altitude (N.M.) = 120,000

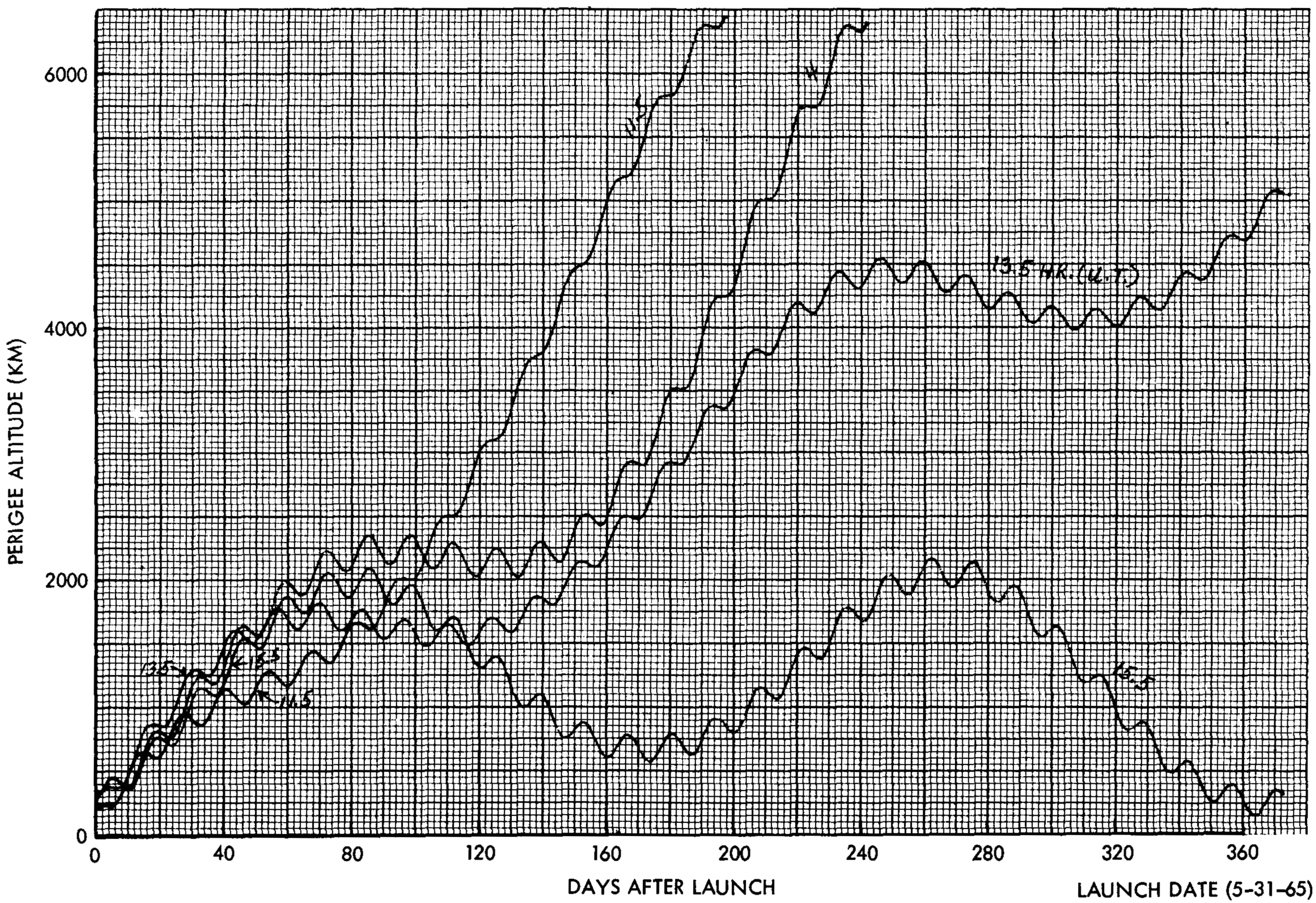

Figure 23—Perigee Height

IMP-B' LAUNCH WINDOW STUDY
Apogee Altitude (N.M.) = 120,000

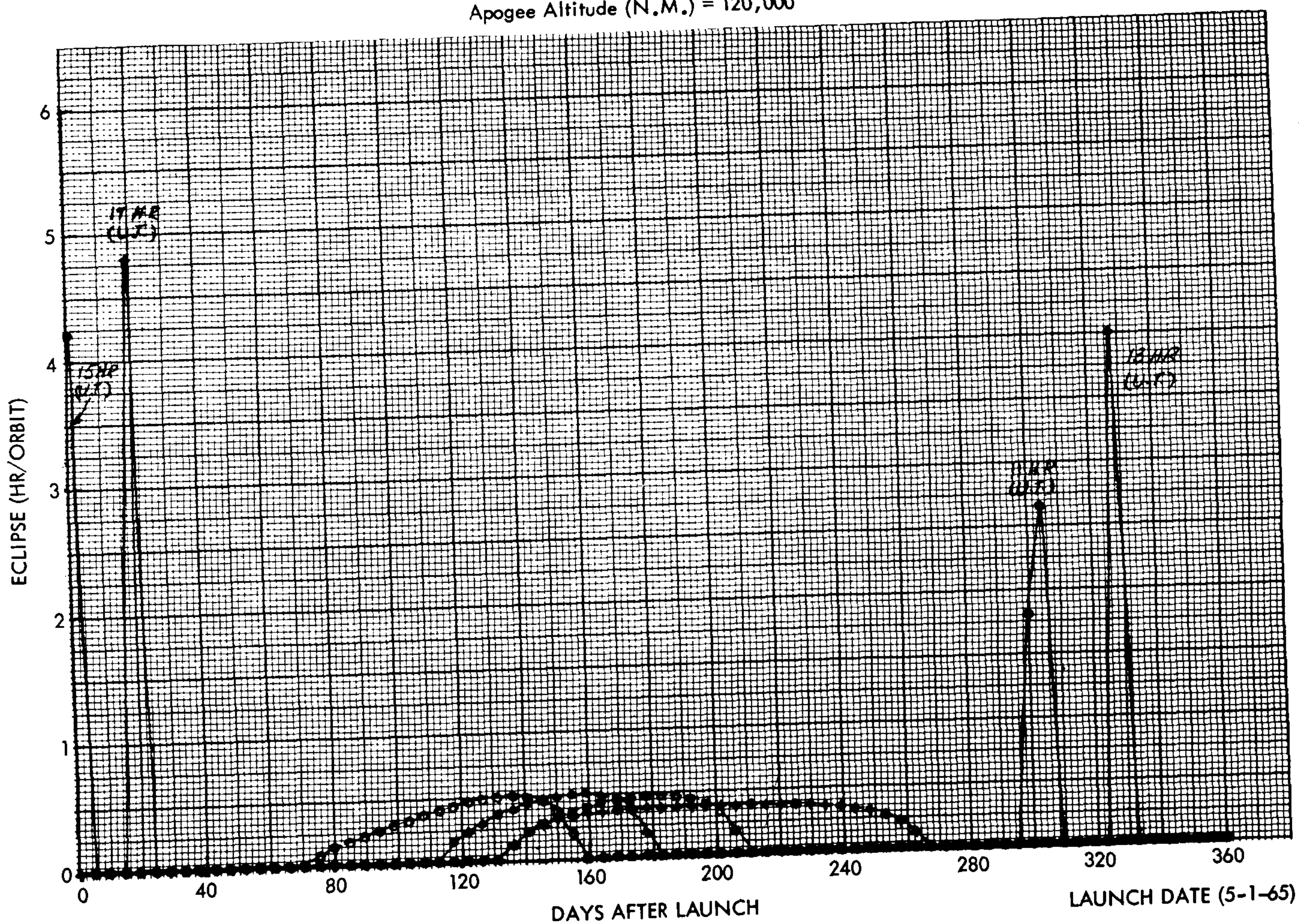

Figure 24–Eclipse Time per Orbit

IMP-B' LAUNCH WINDOW STUDY
Apogee Altitude (N.M.) = 120,000

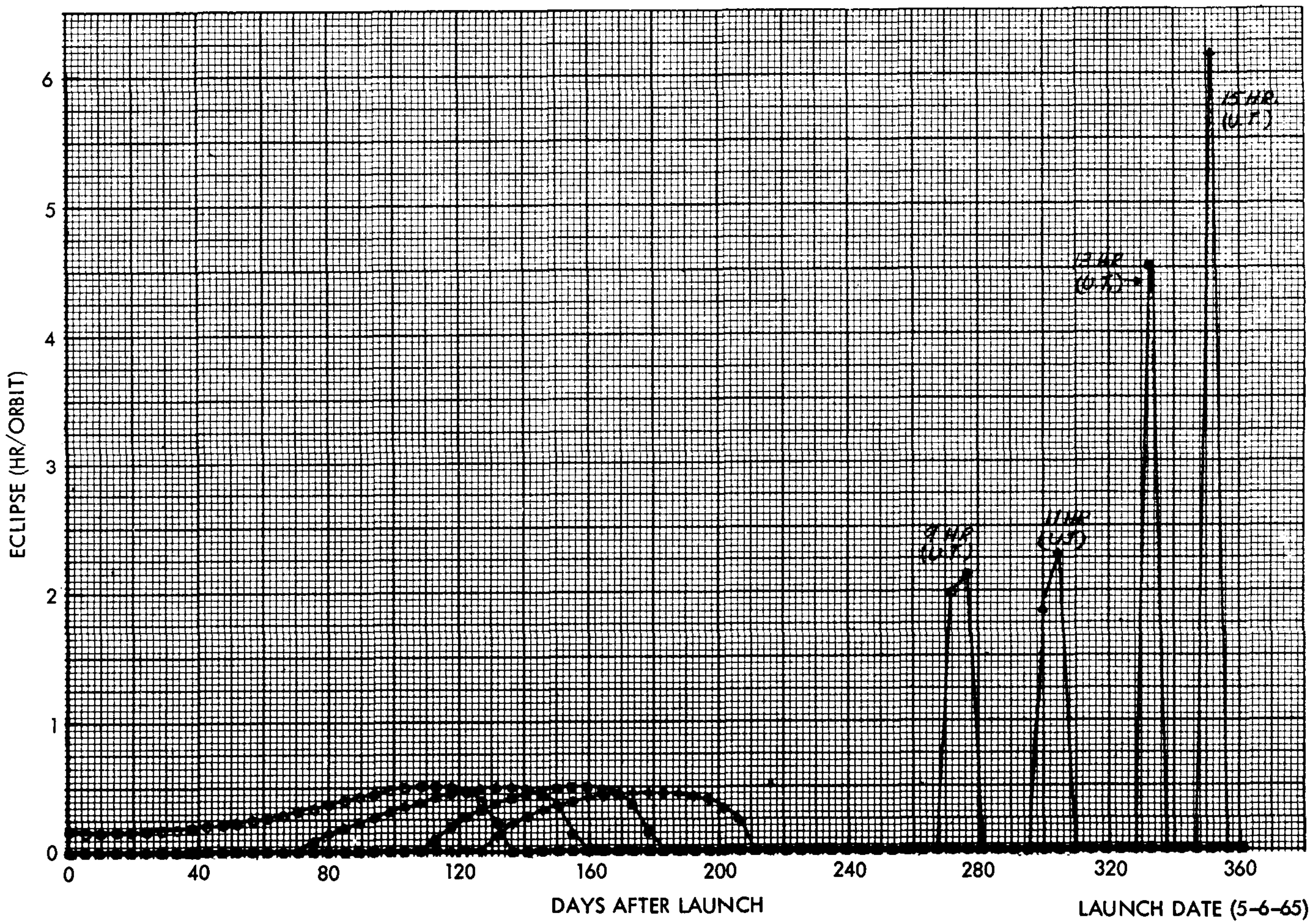

Figure 25–Eclipse Time per Orbit

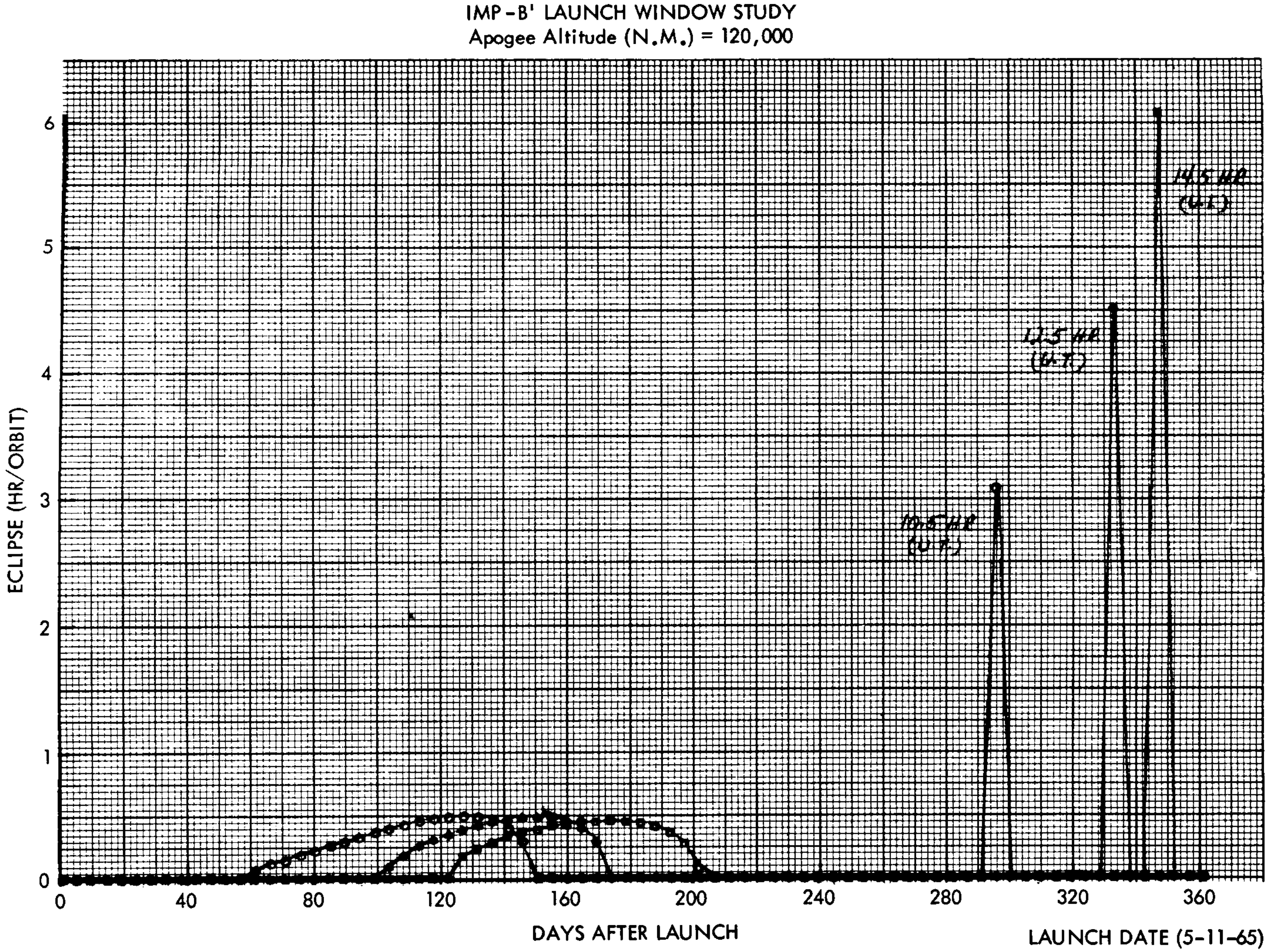

Figure 26–Eclipse Time per Orbit

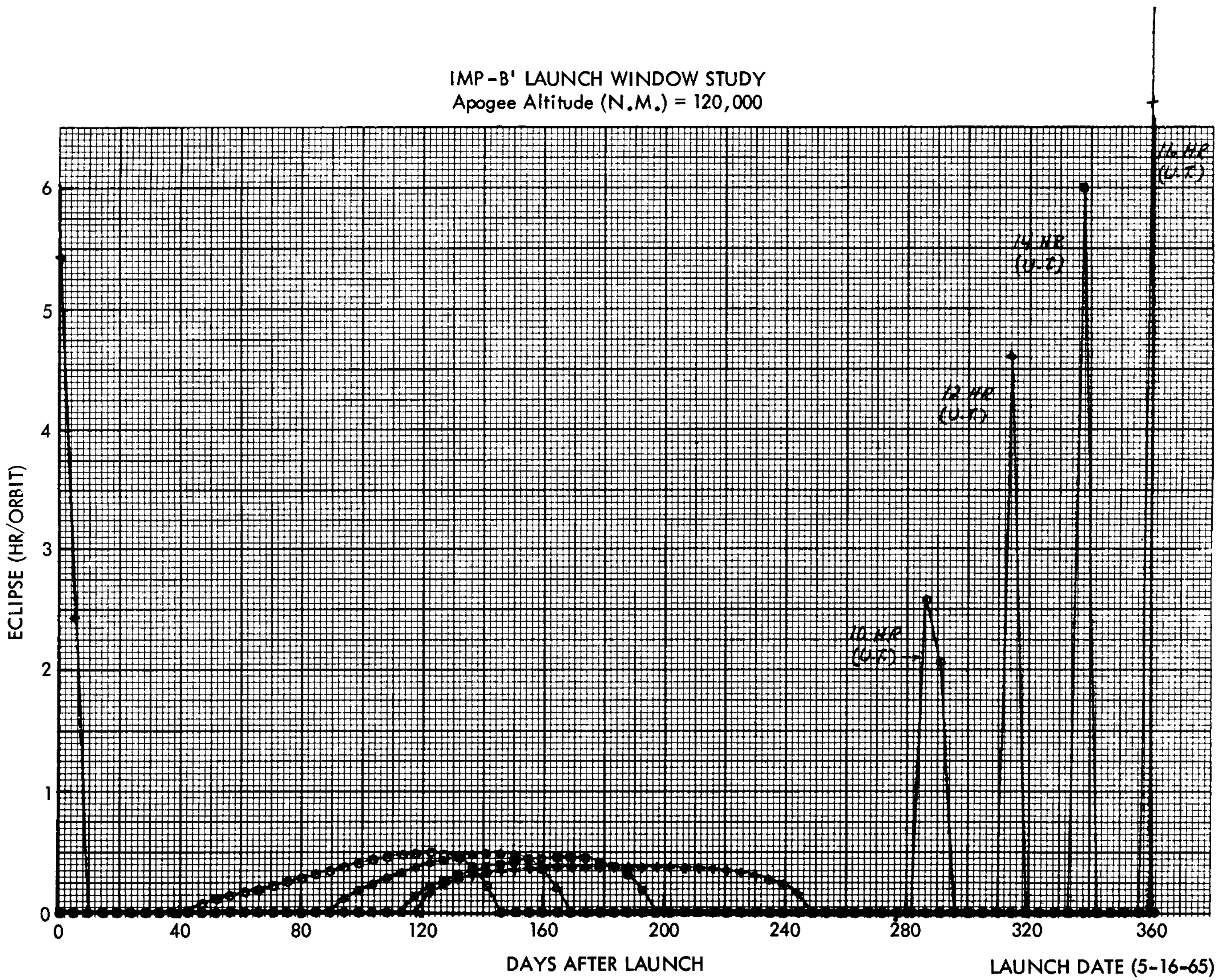

Figure 27—Eclipse Time per Orbit

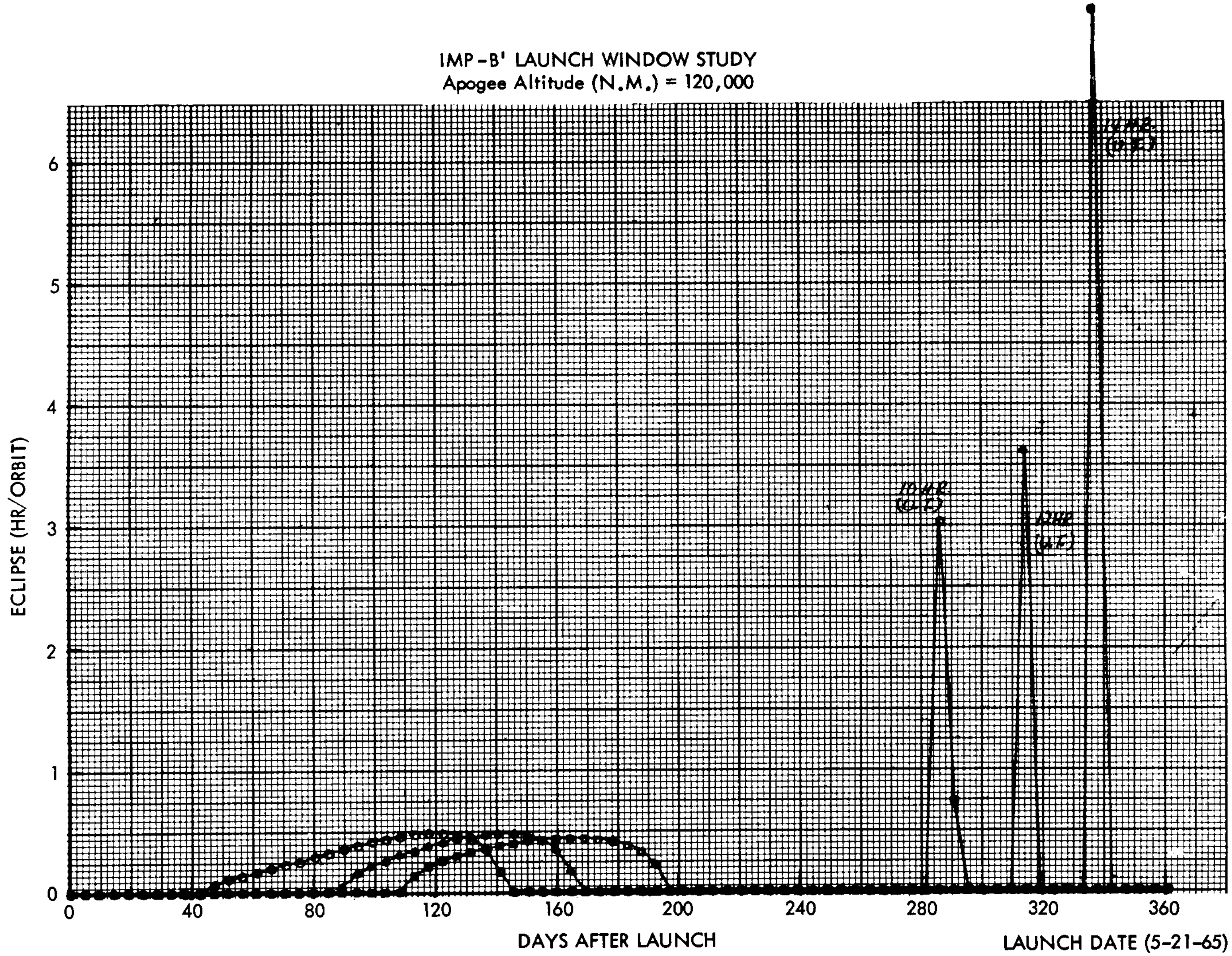

Figure 28–Eclipse Time per Orbit

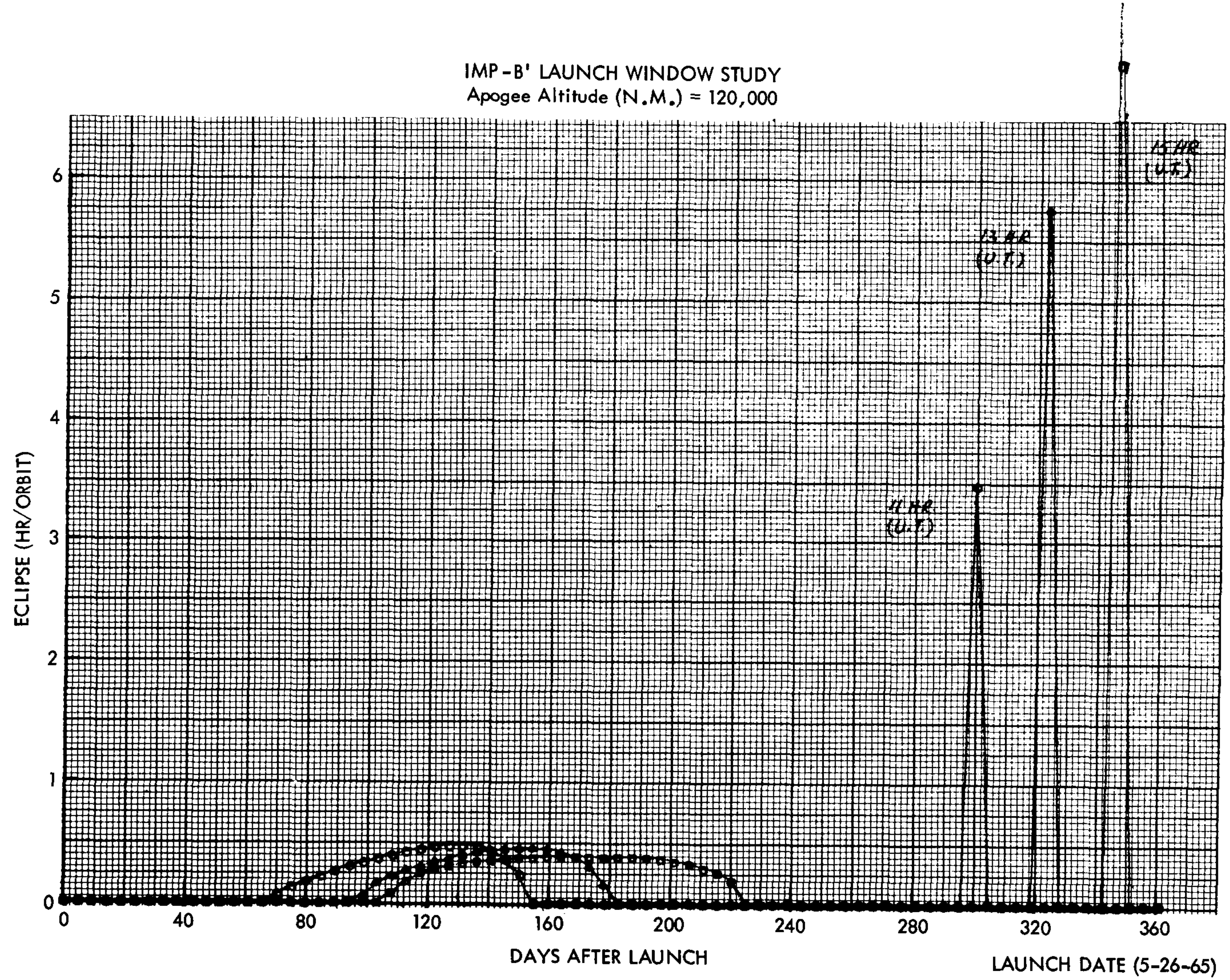

Figure 29–Eclipse Time per Orbit

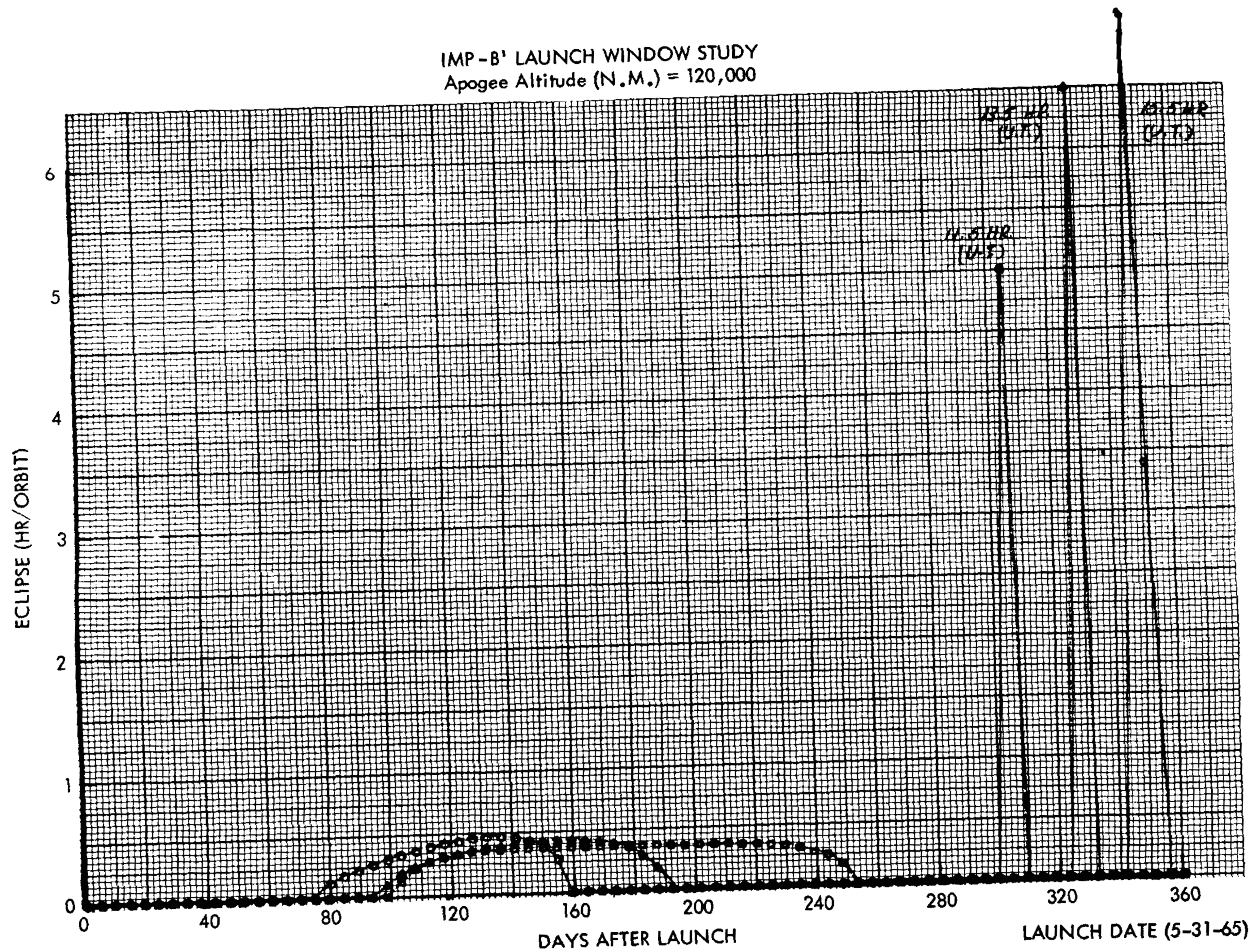

Figure 30–Eclipse Time per Orbit

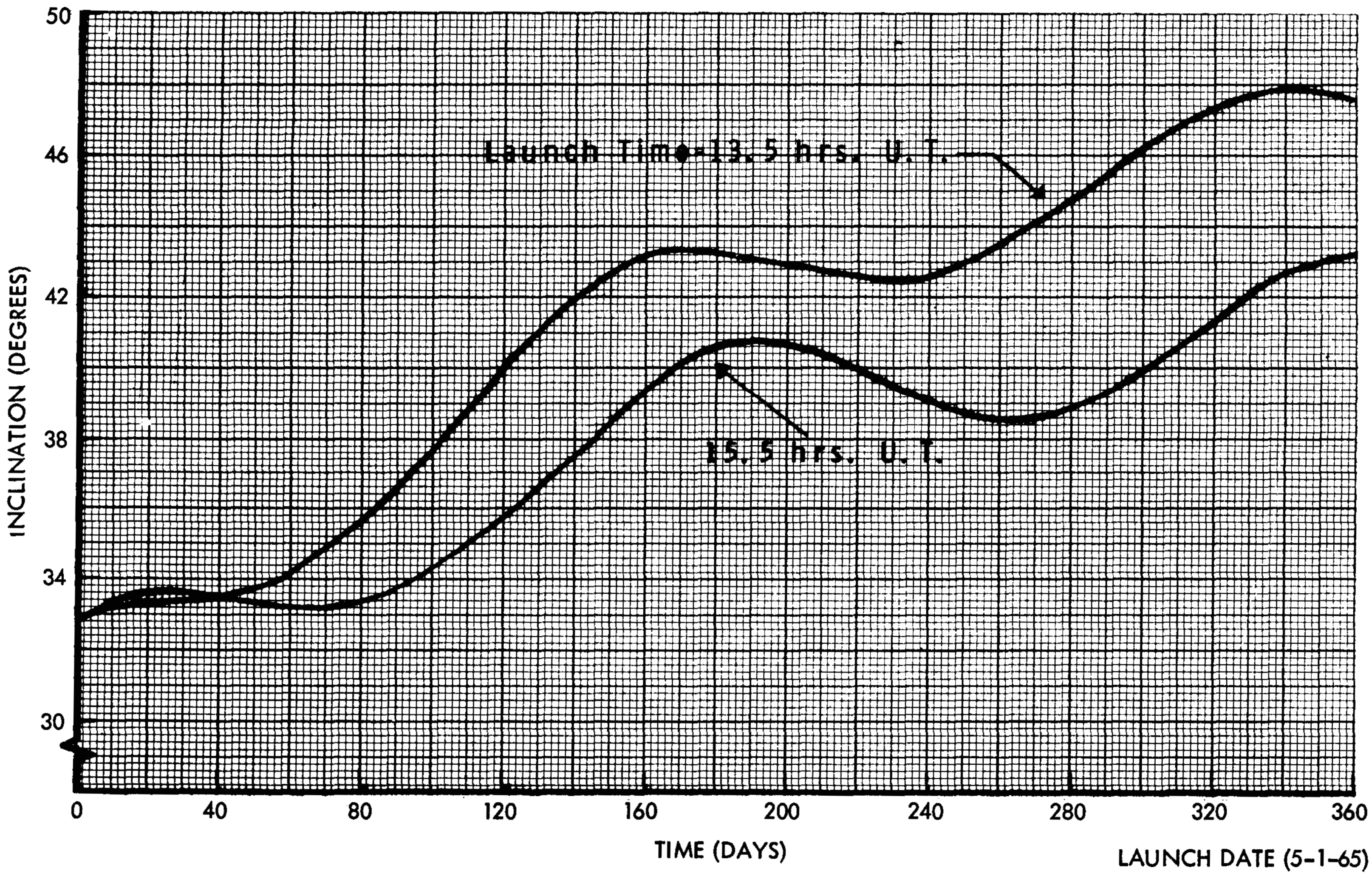

Figure 31–Inclination

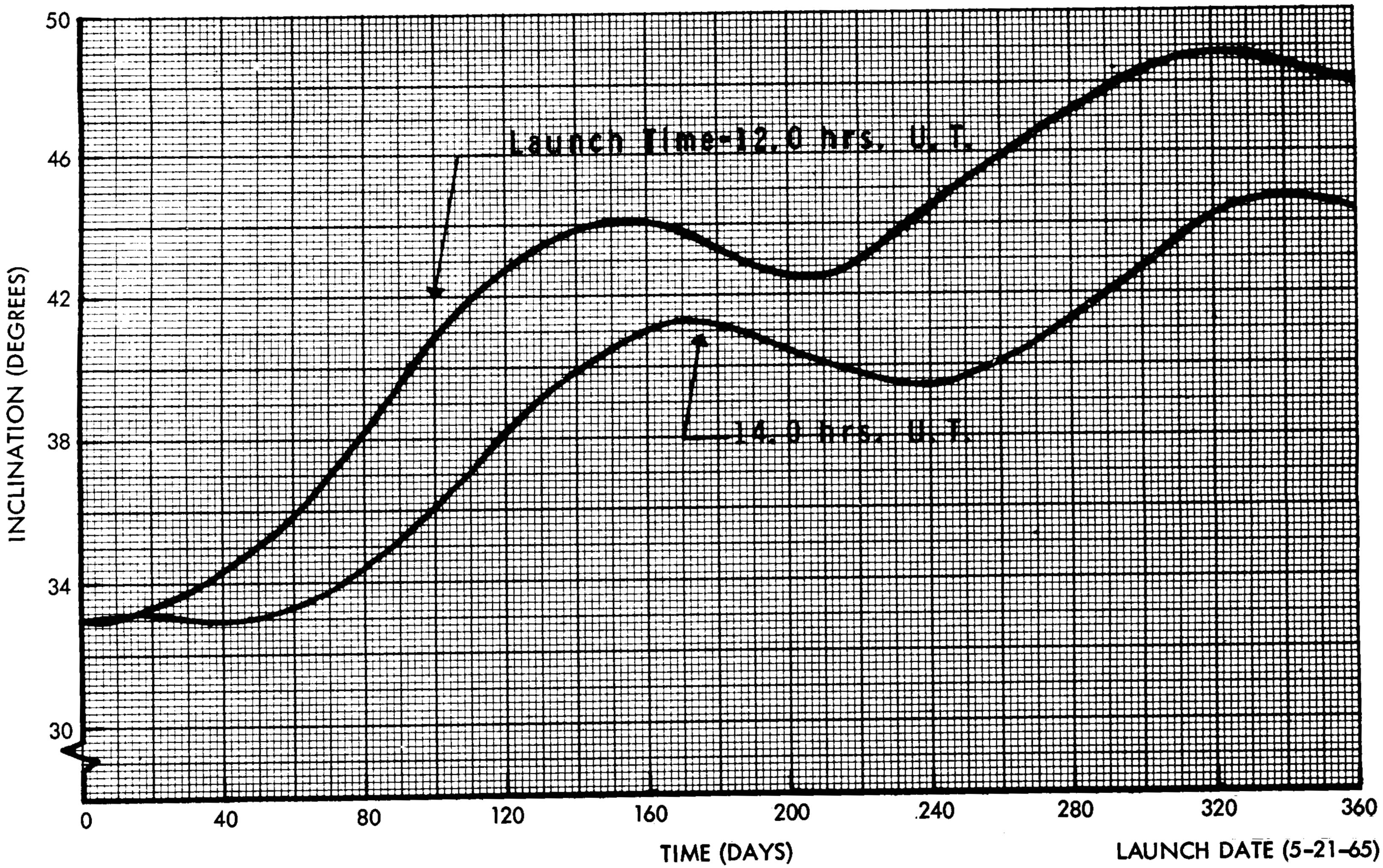

Figure 32–Inclination

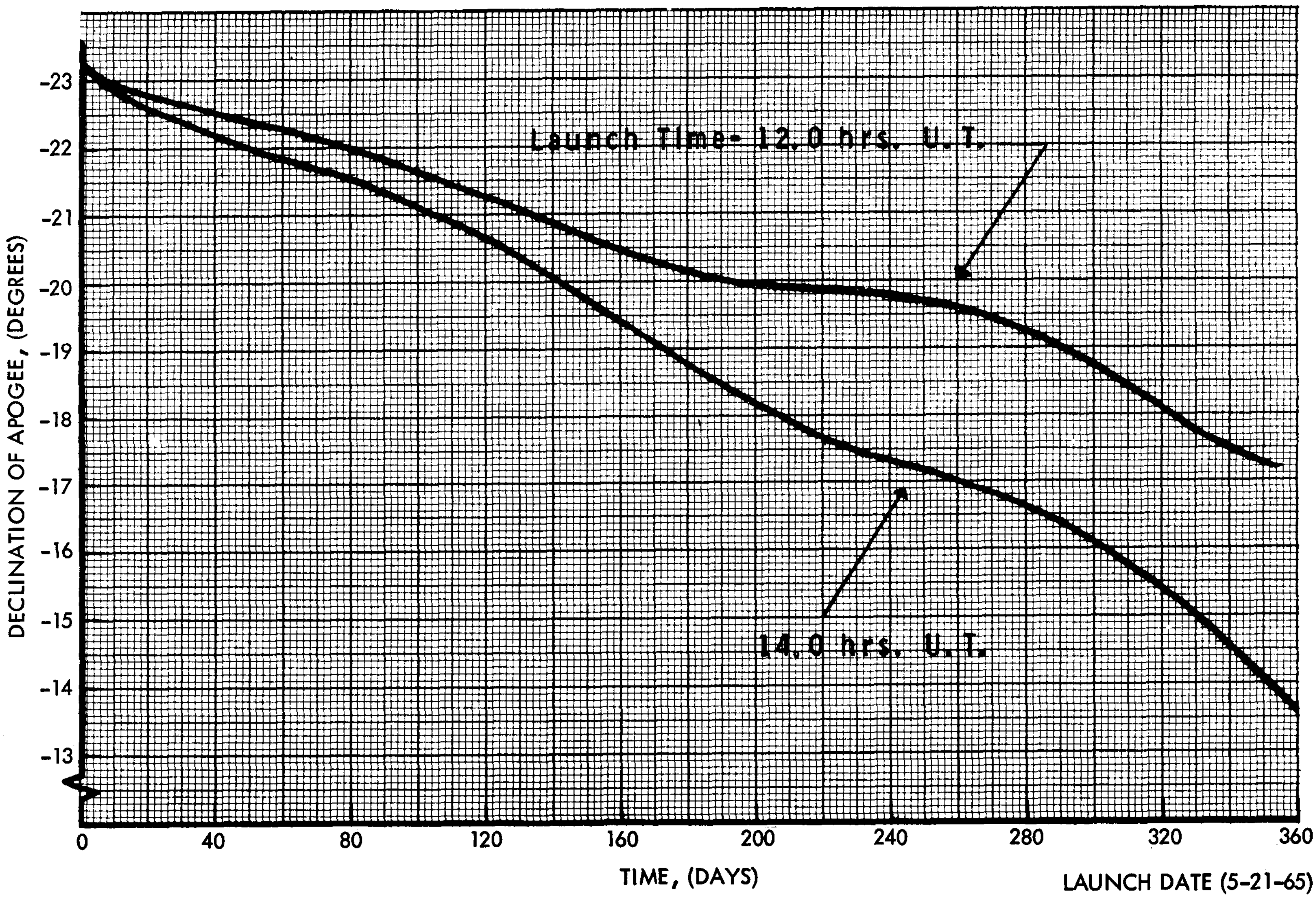

Figure 33–Declination of Apogee

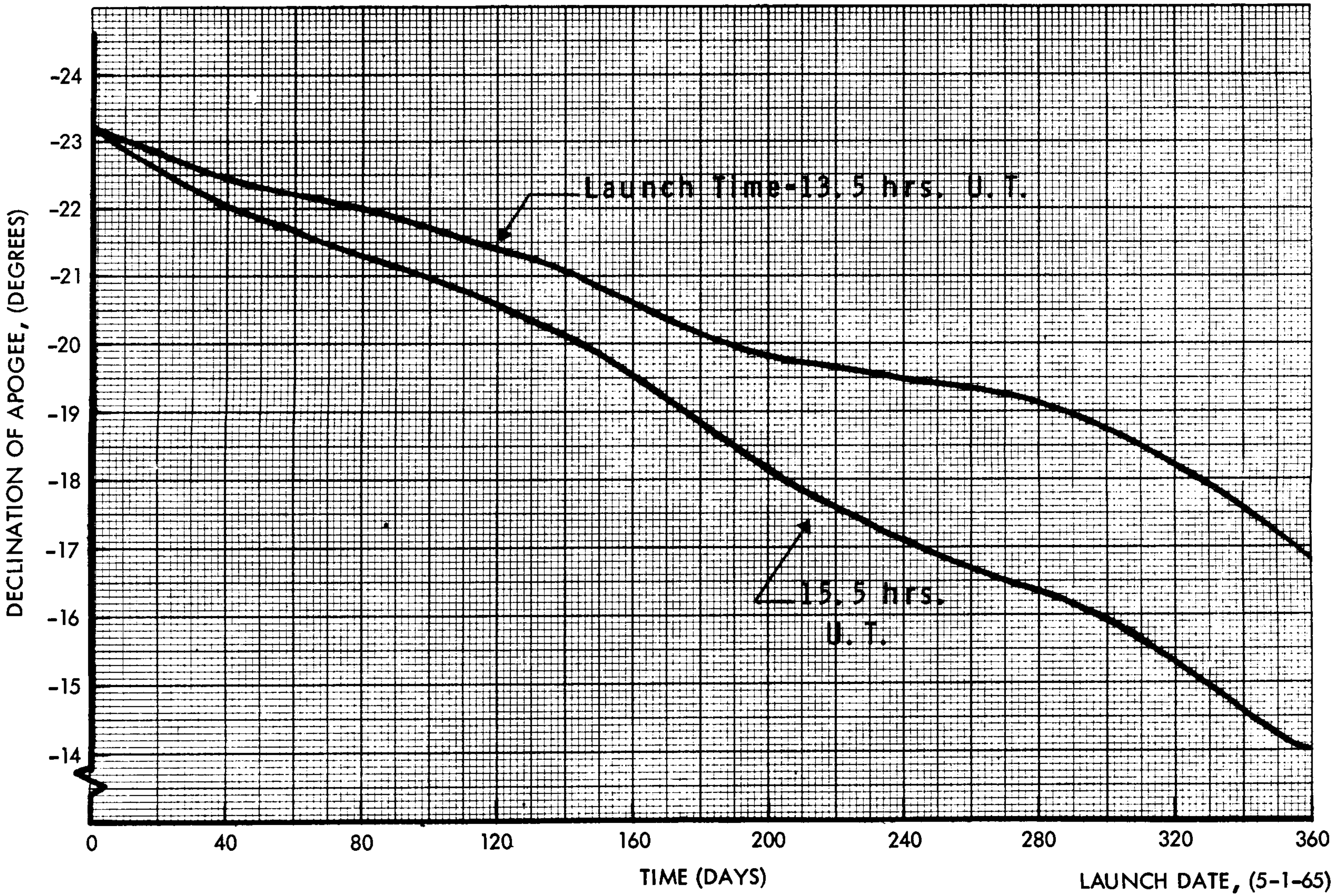

Figure 34–Declination of Apogee